Sled Tests for Development of HIII CAE Dummy Certification Method

Bengt Pipkorn, Manuel Valdano, Martin Östling, Linda Eriksson, Mikael Videby, Francisco López-Valdés

Abstract Virtual testing has been used as complement to mechanical testing in consumer information programs such as European New Car Assessment Program (Euro NCAP) since 2009. Rapid expansion of virtual testing with additional load cases are announced by Euro NCAP and China-NCAP (C-NCAP). For this development validation of the virtual models is an important aspect. Therefore, there is a need for results from tests with clear and well documented boundary conditions that can be used for validation of the virtual models. For this purpose, tests were carried out with the generic frontal impact sled test set-up at 40kph and 56kph impact velocity with the 5%, 50% and 95% anthropometric test devices (ATD) positioned as drivers. Per each ATD size and crash pulse, 3 repeated tests were run resulting in a total of 18 tests. Prior to test, the position of the ATD was 3D-scanned to enable detailed comparison of the initial position between the physical and CAE ATD model.

Generally small variability in the test results was observed for the tests performed in the same configuration. All ATD readings were higher for the impact at 56kph than for the 40kph impact. Coefficient of variation (CV) rated all (50) but 16 measurements as excellent. Making it an adequate dataset for model validation.

Keywords Virtual testing, validation, 5%HIII, 50%HIII, 95%HIII

I. INTRODUCTION

Numerical simulations have been used in the automotive industry for product development for decades. Using numerical simulations in consumer information programs for vehicle rating is more recent and started in 2009 when the European New Car Assessment Program (Euro NCAP) introduced virtual testing for pedestrian protection [1]. In 2023, a new development regarding the use of virtual testing was announced. The Euro NCAP Far-side occupant assessment was selected as the pilot case for this step [2]. The assessment is aimed at enhancing robustness through the use of WorldSID models. It will be applied for monitoring from 2024 onwards and fully in force from 2026 onwards.

Recently Euro NCAP has proposed the frontal impact Virtual Testing Crashworthiness (VTC), procedure to add more robustness to the evaluation of frontal protection through the deployment of additional, virtual (Computer Aided Engineering) CAE simulations [3]. These simulations will be based on load case variations of the Euro NCAP frontal sled procedure defined in the Euro NCAP Frontal Occupant Test & Assessment protocol [4 and 5]. The family of adult HIII anthropometric test device (ATD) models are included to address the influence of occupant variability in occupant protection.

For successful virtual testing robust, reliable, and thoroughly validated occupant models that meet industry expectations is a key aspect. Models to be used for virtual testing in consumer information programmes have to be certified by a qualification procedure. The models have to be validated at component, sub-assembly and full body level. Validation set ups for thorax and neck validation was presented by Shah et al. [6]. Using the set ups validation of the 50% HIII and 50% THOR ATD models was assessed. For full body validation boundary conditions (restraint system) similar to the boundary conditions the model will experience in product development or

Bengt Pipkorn is Director of Simulation at Autoliv Research and Adjunct Professor at Chalmers University (+46 733 614441, bengt.pipkorn@autoliv.com). M. Valdano (e-mail: mvaldano@comillas.edu; tel: +34 644 64 05 53) is a PhD. Student, Martin Östling is a Senior Research Specialist at Autoliv Research, Vårgårda, Sweden. Linda Eriksson is a Senior CAE specialist at Autoliv Sweden, Vårgårda, Sweden, Mikael Videby is a Senior System Engineer at Autoliv Sweden, Vårgårda, Sweden and F. J. López-Valdés is an Associate Professor and Researcher at MOBIOS, IIT, Universidad Pontificia Comillas, Madrid.

consumer information program evaluations is necessary. In parallel, to enable the development of robust and reliable virtual models of the boundary conditions, they have to be clear and simple (as straightforward as possible). The relevant boundary conditions necessary to describe the loading environment in a sled set up are the seat, the seat belt system and the airbag. In the past sled tests were carried out for validation of the 5% and 50% HIII ATD by Automotive Occupant Restraints Council (AROC) [7]. However, the boundary conditions used in the test setup were not clear and limited results from the tests were published. Therefore, there is a need for sled test data in a simple generic environment with clear boundary conditions that can be used to validate the HIII family of ATD models.

The objective of the study is to use a simplified frontal impact sled test environment and to generate sled test results with the adult family of HIII ATDs and make the sled environment and test results publicly available for development of HII ATD model certification procedure.

II. METHODS

For a consumer rating programme, it is essential that Euro NCAP has full confidence in the models used for evaluation. To ensure that simulation predictions are trustworthy, robust, reliable and can be applied practically to the different assessments a simple validation case for the 5%, 50% and 95% HIII ATD models is presented.

The validation case consists of results from tests with a generic frontal impact sled (Fig. 1). The sled was comprising of generic floor pan, generic foot support, rigid and padded seat-back (support the occupant prior crash), semi rigid seat [8], 3-pt seat belt system, shoulder belt retractor with 2kN pretensioner and 4kN load limiter, seat belt buckle with wire stalk, crash-locking tongue, and 2kN lap belt pretensioner, generic knee bolster, collapsible steering column, steering wheel and driver airbag [9]. Steering wheel and steering column angle can be found in appendix A. The width of the seatbelt webbing (Rukaflex) was 47mm with a tension of 11,5kN at 10% elongation. The semi rigid seat was consisting of a seat pan and sub pan. The seat pan spring stiffness was 128N/mm, and sub pan springs stiffness were 132N/mm. Seat pan, sub pan and seatback angles can be found in appendix A. A 45°-foot support were also included. The generic sled was mimicking mid-size European vehicles.

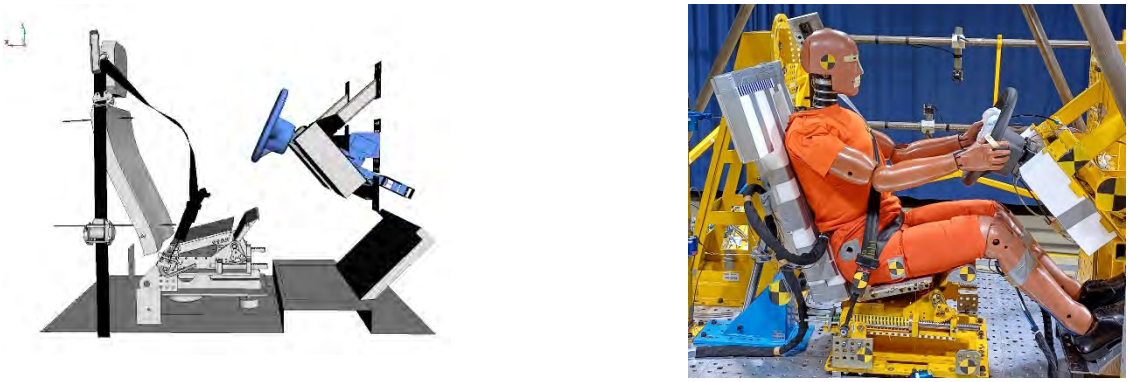

Fig. 1. Generic Frontal System Model

The coordinates for the retractor and D-loop of the belt system were based on a European mid size sedan vehicle geometry. The generic knee bolster was rectangular (300 x 230 x 100mm) Ethafoam 220 blocks. The steering column deformation force was controlled by deforming steel elements. The element used for the testing were 350 x 2 x 23 mm SSAB Domex 420LA steel elements resulting in a deformation force of approximately 5.5kN with max deformation distance of 85mm.

The steering wheel was from a Volvo XC90 MY 2021. The generic airbag was a single chamber, coated fabric 55 litre bag with 2 x35mm diameter went holes. There was no cover over the airbag and the bag was fixated with paper tape. The inflator used was a pyrotechnic 2 stage gasgenerator.

In all tests the retractor pretensioner was fired at 10ms, the anchor plate pretensioner at 15ms while airbag stage one was fired at 10ms and stage 2 at 15ms.

Two different impact velocities were used corresponding to full frontal rigid barrier impacts at 40 and 56kph (Fig. 2) [10]. Peak acceleration for the pulses were 27 and 37g respectively. Three repeated tests with each of the 5%, 50% and 95% HIII ATDs were carried out resulting in a total of 18 tests.

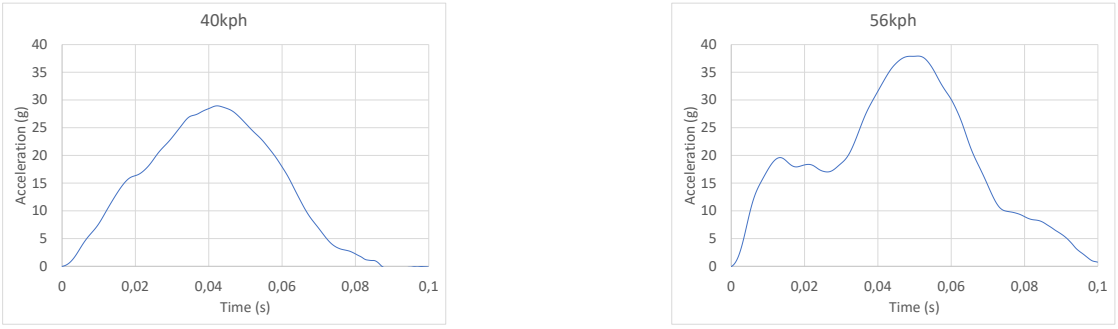

Fig. 2. 40kph and 56kph Crash Pulses

On the generic frontal impact sled belt pull and pay out, force at retractor (B1) (middle between retractor and D-Loop), force at shoulder (B3), force at end bracket (B6) were recorded (Table 1). Airbag pressure, steering column deformation force and displacement, seat pan displacement and sled acceleration were also recorded. Sled transducer type and manufacturer can be found in appendix B.

Table 1
Sled Measurements

Transducer	**Measurement**
Belt force at retractor (B1)	F
Belt force at shoulder (B3)	F
Belt force at end bracket (B6)	F
Belt pay in and pull out	D
Airbag pressure	P
Steering column force	F
Steering column displacement	D
Seat pan displacement	Dz
Sled acceleration	Ax

For all ATDs head acceleration, head rotational velocity, upper neck force and moment, T1 displacement, chest deflection, chest acceleration, sternum acceleration, pelvis acceleration, pelvis displacement, pelvis rotational velocity, lumbar spine force and moment were measured (Table 2). T1 and pelvis displacements were recorded by means of a string potentiometer that was attached to the T1 and pelvis of the ATD and a rigid point on the sled (Fig. 3).

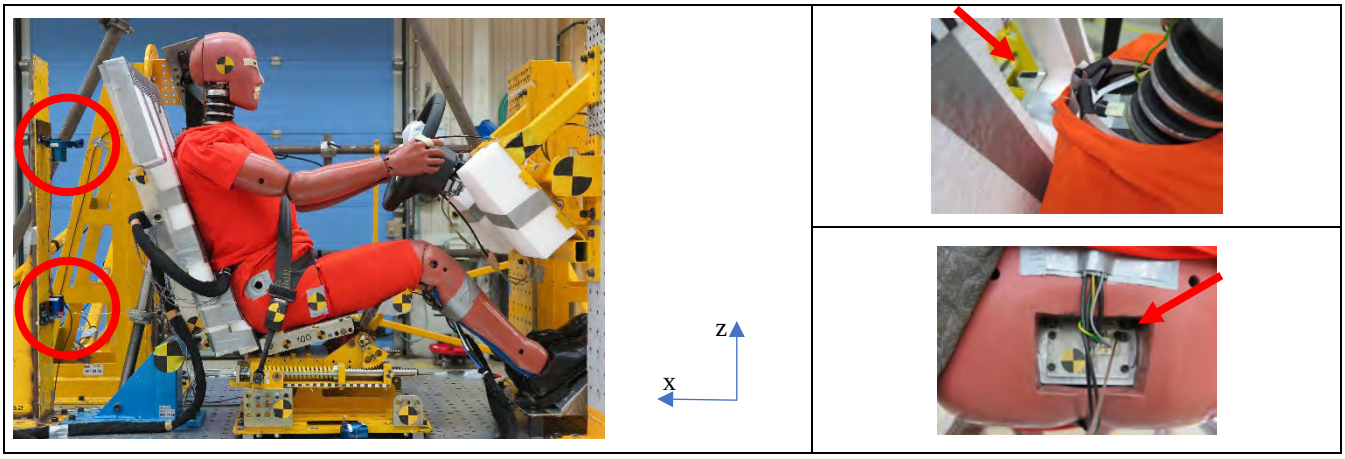

Fig. 3. String potentiometer mounting on T1 and pelvis

Table 2
ATD Measurements

Transducer	Axis	Measurement	5% HIII	HIII 50%	HIII 95%
Head Accelerometer	X-, Y-, Z-	Ax, Ay, Az	X	X	X
Head Gyro	X-, Y-, Z-	ωx, ωy, ωz	X	X	X
Upper Neck	X-, Y-, Z-	Fx, Fy, Fz, Mx, My, Mz	X	X	X
Chest Deflection	-	D	X	X	X
Chest Acceleration	X-, Y-, Z-	Ax, Ay, Az	X	X	X
Lumbar Spine	X-, Y-, Z-	Fx, Fz, My	X	X	X
Pelvis Accelerometer	X-, Y-, Z-	Ax, Ay, Az	X	X	X
Pelvis Gyro	Y-	ωy	X	X	X
Femur	-	F	X	X	X
T1	-	D	X	X	X
Pelvis	-	D	X	X	X

Seat coordinate system origin was defined as the rear right corner of seat frame (origo). The tests were conducted using three HIII ATDs, 5%, 50% and 95% manufactured by Humanetics [11]. The ATDs were seated in an upright posture with their hands on the steering wheel. The 50% HIII ATD was positioned with the H-point 103mm forward (x-dir) and 159mm above (z-dir) the origin. The 95% HIII ATD was positioned 108mm forward (x-dir) and 168mm above (z-dir) the origin. When positioning a close match to the target coordinates was achieved. Target coordinates with tolerances and how much the individual tests differed from the target values are provided in appendix C. Upper steering wheel rim to nose, shoulder belt to mouth and shoulder belt to neck measurements can be found in appendix D.

For the 5% HIII ATD the seat was moved 100mm forward and 25mm upwards from the HIII seat position (including origin). The foot support was moved 40mm rearwards (x-dir) and 22mm upwards (z-dir). The ATD was positioned with the H-point 120mm forward (x-dir) and 167mm above the origin.

Onboard high-speed cameras recorded the tests at a frequency of 1000Hz. These cameras captured images of the left and right-side overview, a top and front view, and detailed views of the pelvis and its interaction with the seat, lap belt, lap belt pre-tensioner, buckle, and crash locking tongue. All measurements were filtered according to Euro NCAP Technical bulletin, TB 021 [12].

A traditional method for assessing the repeatability of the ATD responses was used. The mean ($\bar{X}$), the standard deviation (σ), and the coefficient of variation (CV) of the peak response parameters was quantified [13]. To be consistent the peak absolute value of the response and a 140ms time corridor was selected for the assessment. Historically National Highway Traffic Safety Administration (NHTSA) has categorized a CV between

0-5% to be excellent, 5-8% to be good, 8-10% to be acceptable and >10% to be unacceptable was used to judge the repeatability [13].

$$CV = \frac{\sigma}{\bar{X}} \text{ x } 100\% \quad (1)$$

III. RESULTS

Prior to test, the position of the ATD was 3D-scanned (Fig. 4). The 3D scan can be superposed on the CAE ATD to enable detailed positioning and accurate replication of the belt routing across the thorax and pelvis.

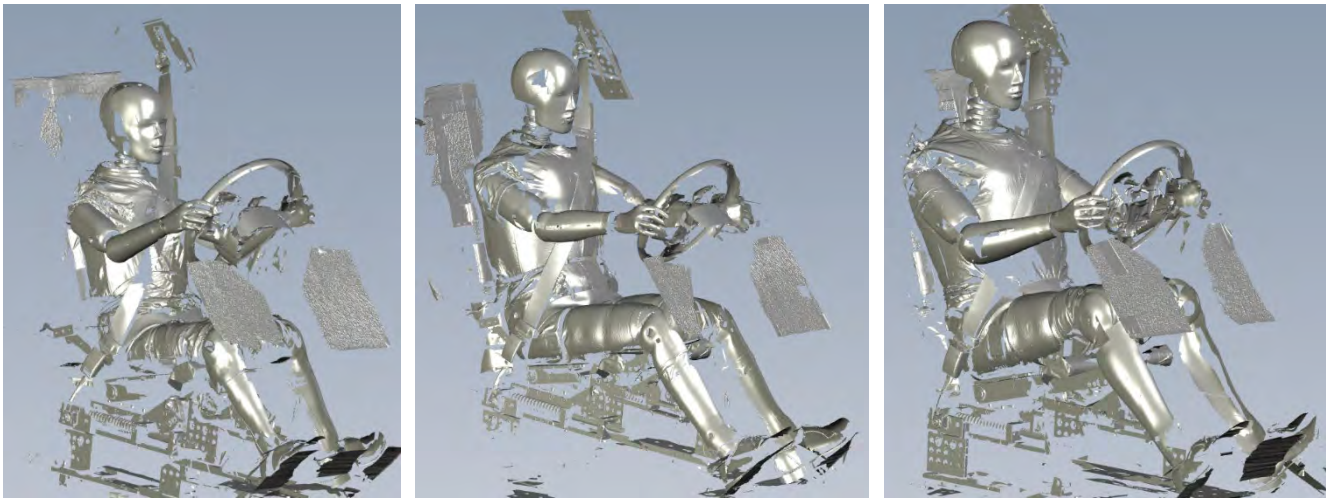

HIII 5% F HIII 50% M HIII 95% M

Fig. 4. 3D-scan 5%, 50% and 95% HIII pre-test posture

The individual measurements for the repeated tests are presented in the appendix. In appendix E the results from the 5% HIII ATD are presented, in appendix F the results from the 50% HIII ATD and in appendix G the results from the 95% HIII ATD.

For the 40kph crash pulse peak acceleration was 29g and for the 56kph crash pulse peak acceleration was 38g (Fig. **5**). CV was very small, and all pulses were rated as excellent.

	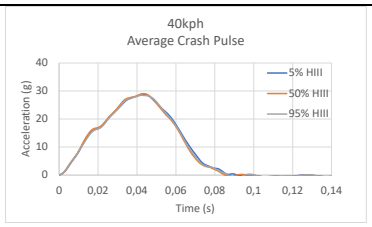	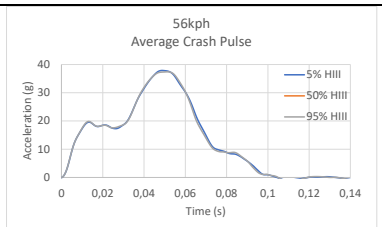
CV	5%HIII:0%, 50%HIII:1%, 95%HIII:1%	5%HIII:0%, 50%HIII:0%, 95%HIII:0%

Fig. 5. Average Crash Pulses

For all three dummies the same amount of belt (~70mm) was pulled in by the retractor for both the 40 and 56kph impacts. For the 95%, 50% and 5% HIII 139, 100 and 25mm belt was pulled out respectively (Fig. 6). In the 56 kph impact 240, 200 and 90mm belt was pulled out for the 95%, 50% and 5% HIII dummies respectively. In both the 40kph and 56kph impacts shoulder belt forces were similar. Peak shoulder belt force varied from 5000N for the 95% HIII to 4000N for the 5% HIII ATD. The lap belt force due to the lap belt pretensioner was 2000N for the 5%, 50% and 95% HIII ATDs. In the 40kph impact peak lap belt force was 8200, 7000 and 4000N for the 95%, 50% and 5% HIII ATDs. In the 56kph impact peak lap belt force was 11000, 10000 and 5000N for the 95%, 50% and 5% HIII ATDs respectively.

CV was excellent for all measurements, but the retractor pull in/pay out for the 5% HIII and 50% HIII, which were rated as unacceptable and good respectively.

	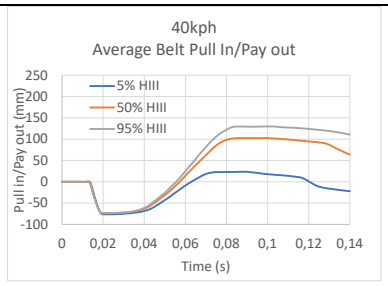	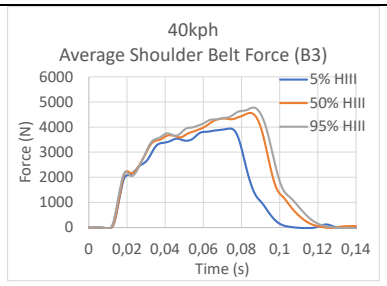	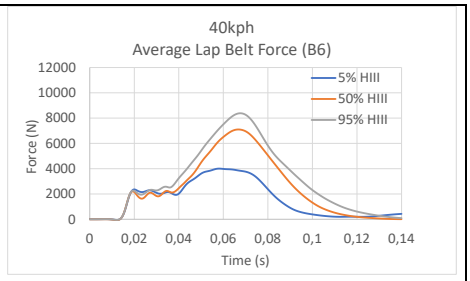
CV	5%HIII:**26%,** 50%HIII:**7%**, 95%HIII:**1%**	5%HIII:1%, 50%HIII:4%, 95%HIII:5%	5%HIII:4%, 50%HIII:1%, 95%HIII:1%
	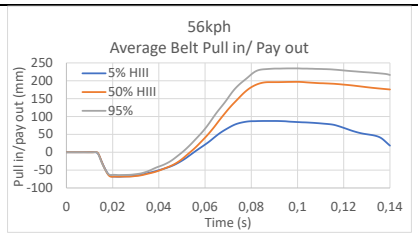	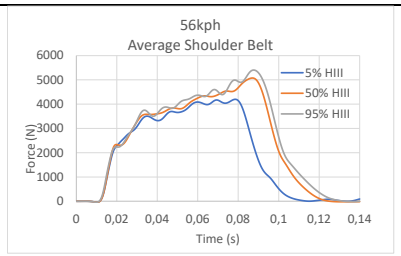	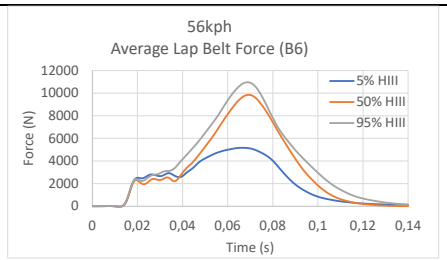
CV	5%HIII:4%, 50%HIII:3%, 95%HIII:1%	5%HIII:3%, 50%HIII:3%, 95%HIII:2%	5%HIII:2%, 50%HIII:1%, 95%HIII:1%

Fig. 6. Average and coefficient of variation belt pull in/pay out, shoulder belt and lap belt force

In the 40kph test steering column displacement was small, less than 20mm for all three dummies while in the 50kph test the displacement was 40mm for the 5% HIII ATD and 80mm for the 95% HIII ATD (Fig. 7). Peak steering column force was between 4 -5kN for all three dummies in the 40kph test and between 5-6kN in the 56kph test. Peak airbag working pressure (when the bag was loaded by the ATD) was ~30kPa for all three dummies in the 40kph tests and 35-40kPa in the 56kph tests. Seat pan displacement (string potentiometer located in the front part of the seat pan) was 12mm for the 5% HIII, 35mm for the 50% HIII and 39mm for the 95% HIII ATD in the 40kph test. In the 56 kph test the displacement was 20mm for the 5% HIII, 33mm for the 50% HIII and 34mm for the 95% HIII ATDs.

CV was excellent for all measurements but steering column displacement. In the 40kph test CV was good for the 5% HIII and 95% HIII and unacceptable for the 50% HIII dummies. In the 56kph test CV was good for the 50% HIII ATD.

	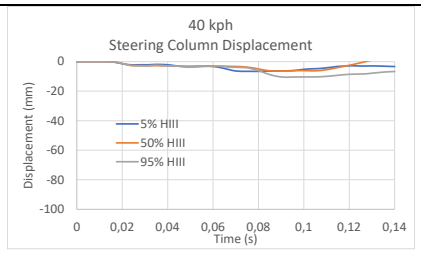	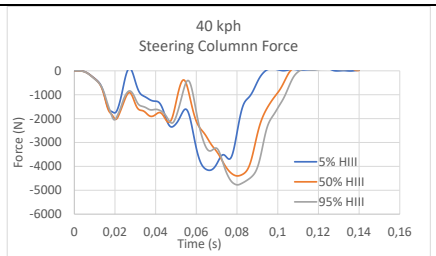	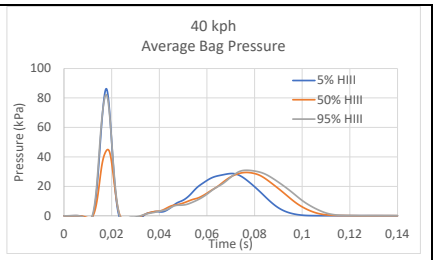
CV	5%HIII:7%, 50%HIII:12%, 95%HIII:8%	5%HIII:2%, 50%HIII:3%, 95%HIII:1%	5%HIII:2%, 50%HIII:2%, 95%HIII:0%
	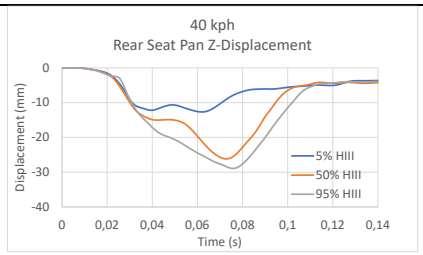		
CV	5%HIII:4%, 50%HIII:2%, 95%HIII:0%		
	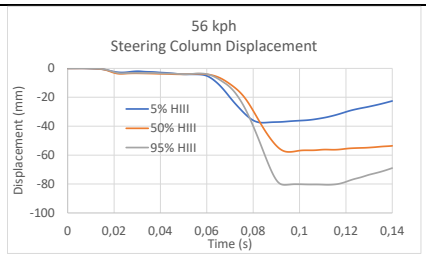	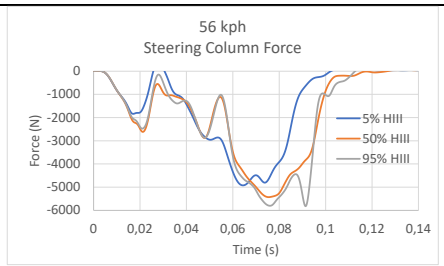	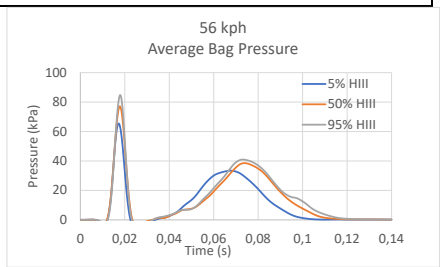
CV	5%HIII:1%, 50%HIII:7%, 95%HIII:0%	5%HIII:0%, 50%HIII:1%, 95%HIII:5%	5%HIII:1%, 50%HIII:1%, 95%HIII:0%
	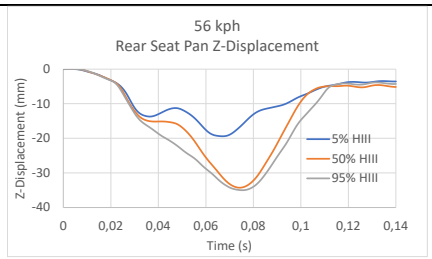		
CV	5%HIII:2%, 50%HIII:1%, 95%HIII:0%		

Fig. 7. Average and coefficient of variation steering column displacement, force, airbag pressure and seat pan displacement

Peak head resultant acceleration varied between 41-49g in the 40kph test and from 53-66g in the 56kph test for the three dummies (Fig. 8). Peak head angular velocity varied from -900deg/s to -1000deg/s to -1200deg/s for the 5%, 50% and 95% HIII ATD respectively in the 40kph test. In the 56kph test peak head angular velocity varied from 1200deg/s to -1500deg/s to -2100deg/s for the 5%, 50% and 95% HIII ATD respectively. Peak head displacement varied from 300mm to 500mm respectively for the 5% HIII and 95% HIII in the 40kph test. In the 56kph test peak head displacement varied from 359mm for the 5% HIII to 620mm for the 95% HIII.

CV was excellent for all measurements but for Resulting head acceleration and head y-angular velocity for the 95%HIII in the 40kph tests for which CV was good.

	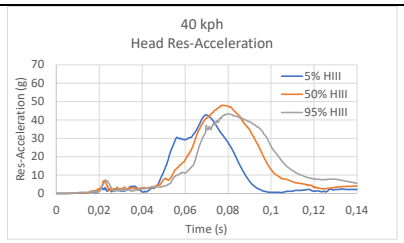	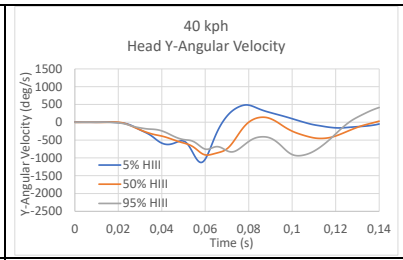	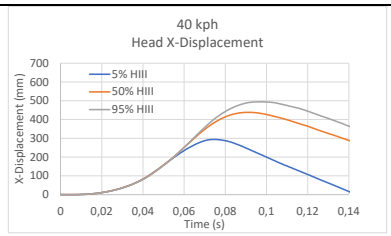
CV	5%HIII:2%, 50%HIII:1%, 95%HIII:6%	5%HIII:2%, 50%HIII:2%, 95%HIII:7%	5%HIII:3%, 50%HIII:1%, 95%HIII:0%
	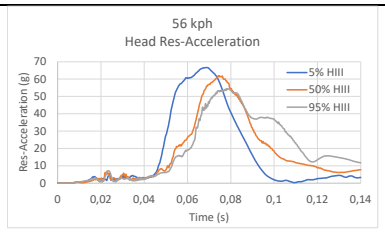	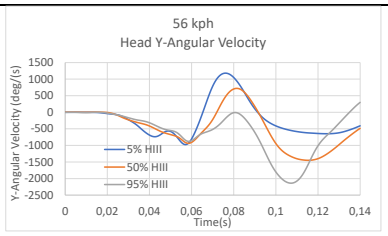	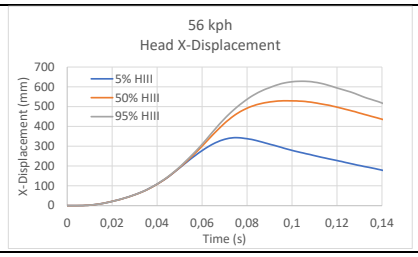
CV	5%HIII:1%, 50%HIII:2%, 95%HIII:2%	5%HIII:3%, 50%HIII:4%, 95%HIII:1%	5%HIII:3%, 50%HIII:0%, 95%HIII:1%

Fig. 8. Average and coefficient of variation head resultant acceleration, angular velocity and x-displacement

The peak upper neck x-forces varied between 430-500N in the 40kph impact test and between 590-700N for the 56kph impact test for all three dummies (Fig. 9). The peak upper neck z-force was 500N for the 50% HIII, 1100N for the 5% HIII and 1500N for the 95% HIII ATD in the 40kph test. In the 56kph test peak upper neck z-force varied from 1400N for the 50%HIII to 2600N for the 95% HIII ATD. In the 40kph impact tests peak upper neck y-moment varied between 30-36Nm and in the 56kph impact tests it varied between 30-40Nm for all three dummies.

CV was excellent for all neck measurements but for upper neck y-moment for the 5% HIII ATD for which the CV was good.

	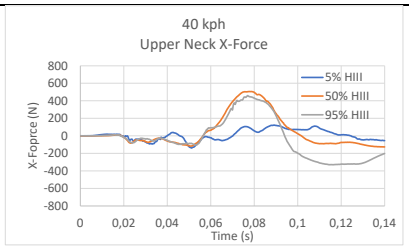	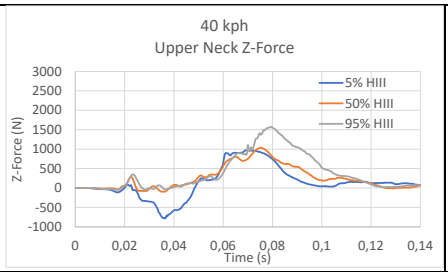	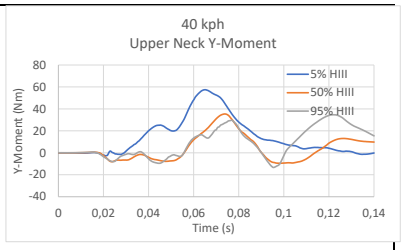
CV	5%HIII:5%, 50%HIII:2%, 95%HIII:5%	5%HIII:6%, 50%HIII:5%, 95%HIII:4%	5%HIII:6%, 50%HIII:5%, 95%HIII:4%
	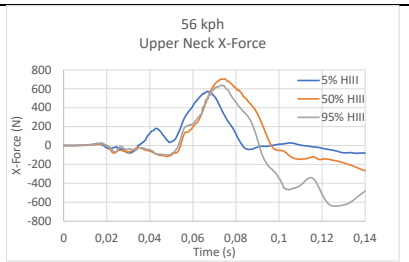	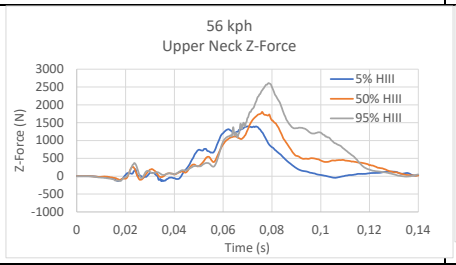	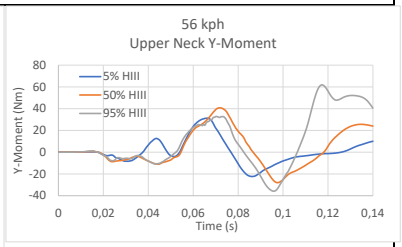
CV	5%HIII:5%, 50%HIII:3%, 95%HIII:5%	5%HIII:1%, 50%HIII:3%, 95%HIII:5%	5%HIII:7%, 50%HIII:5%, 95%HIII:2%

Fig. 9. Average and coefficient of variation upper neck x-force, z-force and y-moment

Peak chest resultant acceleration varied from 35g for the 95% HIII to 38g for the 5%HIII in the 40kph crash (Fig. 10). In the 56kph crash chest resultant acceleration varied from 50g to 53g. Chest deflection varied from 25mm for the 5% HIII ATD to 38mm for the 95% HIII ATD in the 40kph test. In the 56kph test chest deflection varied from 28mm for the 5% HIII ATD to 43mm for the 95% HIII ATD. Peak T1 displacement varied from 250mm for the 5% HIII ATD to 390mm for the 95% HIII ATD in the 40kph crash test. In the 56kph crash test peak lower neck displacement varied from 320mm for the 5%HIII ATD to 500mm for the 50% and 95% HIII ATDs.

CV was excellent for all measurements but chest resultant acceleration for the 5% and 95% HIII ATDs for which CV was good.

	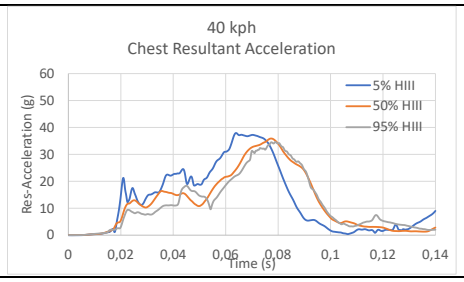	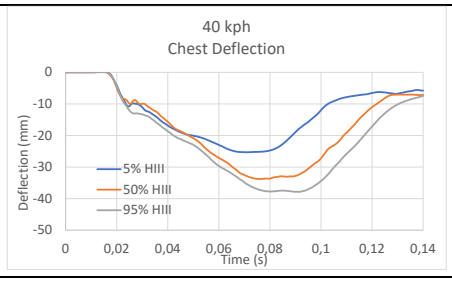	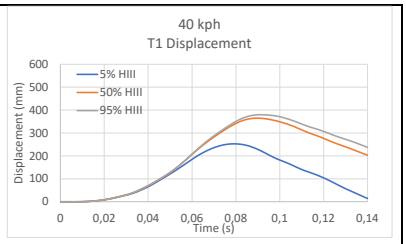
CV	5%HIII:7%, 50%HIII:1%, 95%HIII:8%	5%HIII:2%, 50%HIII:5%, 95%HIII:0%	5%HIII:3%, 50%HIII:2%, 95%HIII:0%
	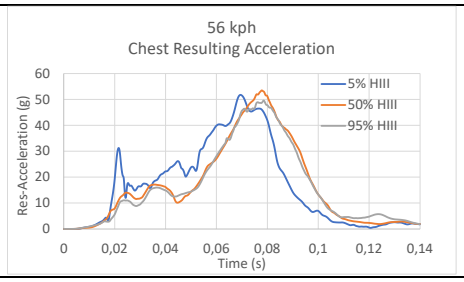	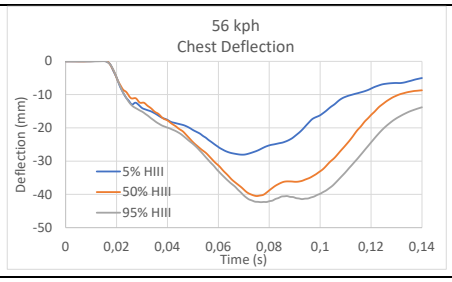	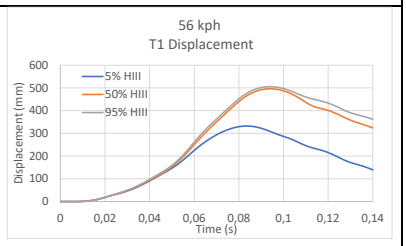
CV	5%HIII:2%, 50%HIII:3%, 95%HIII:3%	5%HIII:0%, 50%HIII:2%, 95%HIII:2%	5%HIII:2%, 50%HIII:2%, 95%HIII:1%

Fig. 10. Average and coefficient of variation chest resultant acceleration, chest deflection, and upper neck displacement

For peak resultant pelvis acceleration, the shape of the 5% HIII ATD varies compared to the shapes of the 50% and 95% HIII ATD acceleration curves (Fig. 11). Peak acceleration in the 40kph test varies from 27g for the 95% HIII ATD to 38g for the 50% HIII ATD in the 40kph impact tests. In the 56kph impact tests pelvis resultant acceleration varies from 40g for the 5% HIII ATD to 65g for the 95% HIII ATD. Peak angular velocity varies from -400deg/s for the 50%HIII and 95% HIII dummies to -560deg/s for the 5% HIII ATD in the 40kph impact tests. In the 56kph impact tests peak angular velocity varies from -400deg/s for the 50% HIII ATD to -700deg/s for the 5% HIII ATD. Peak pelvis displacement varied from 55mm for the 5% HIII ATD to 160mm for the 95% HIII ATD in the 40kph tests. In the 56kph tests pelvis displacement varies from 78mm for the 5% HIII ATD to 198mm for the 95% HIII ATD. CV was excellent for all pelvis measurements.

	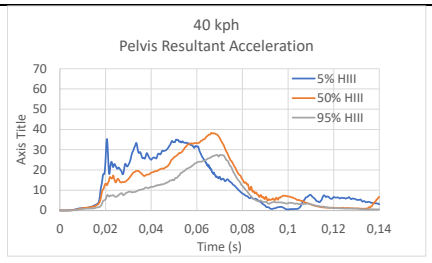	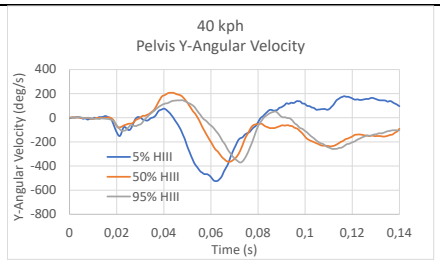	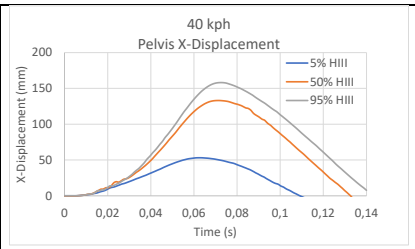
CV	5%HIII:3%, 50%HIII:3%, 95%HIII:2%	5%HIII:4%, 50%HIII:4%, 95%HIII:4%	5%HIII:8%, 50%HIII:1%, 95%HIII:1%
	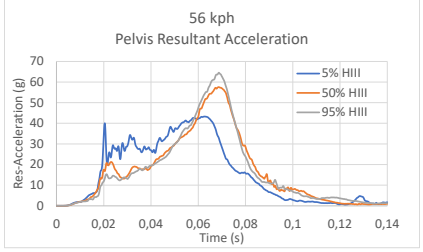	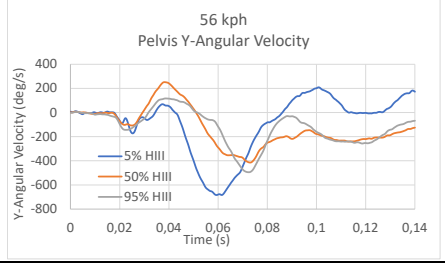	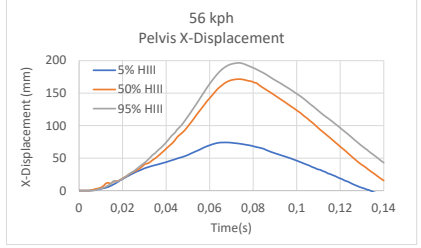
CV	5%HIII:0%, 50%HIII:3%, 95%HIII:1%	5%HIII:3%, 50%HIII:7%, 95%HIII:3%	5%HIII:1%, 50%HIII:1%, 95%HIII:1%

Fig. 11. Average and coefficient of variation pelvis resultant acceleration, angular velocity, displacement, lumbar spine x-force, y-moment

For the lumbar spine measurements, peak x-force varies from -1000N for the 5% HIII ATD to -3200N for the

95% HIII ATD in the 40Kph impact test results (Fig. 12). For the 56kph impact peak lumbar spine x-force varies from -900N for the 5% HIII ATD to -5500N for the 95% HIII ATD. Peak lumbar spine z-force varies from -2000N for the 50% HIII ATD to -1200N for the 95% HIII ATD in the 40kph tests. In the 56kph tests peak lumbar spine z-force varies from -1500N for the 5% HIII ATD to -1100N for the 95% HIII ATD. Peak lumbar spine y-moment varies from 110Nm for the 5% HIII ATD to 410Nm for the 50% HIII ATD in the 40kph tests. In the 56kph tests peak lumbar spine y-moment varies from 140Nm for the 5% HIII ATD to 420Nm for the 95% HIII ATD.

CV was excellent for all measurements but lumbar spine x-force for the 5% HIII ATD in the 40kph impact.

	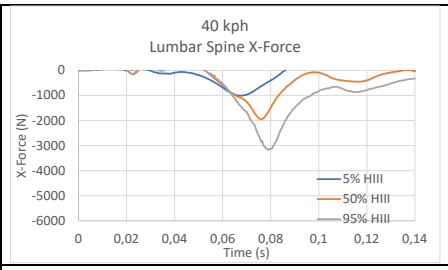	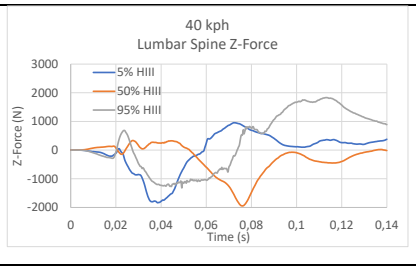	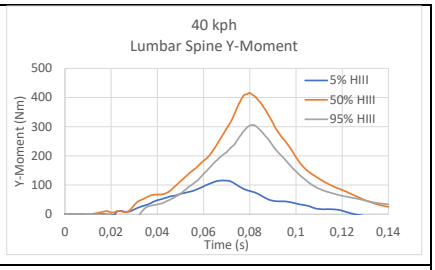
CV	5%HIII:6%, 50%HIII:4%, 95%HIII:5%	5%HIII:2%, 50%HIII:2%, 95%HIII:5%	5%HIII:5%, 50%HIII:1%, 95%HIII:1%
	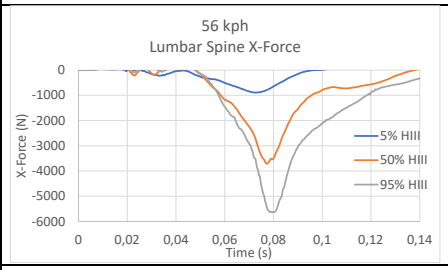	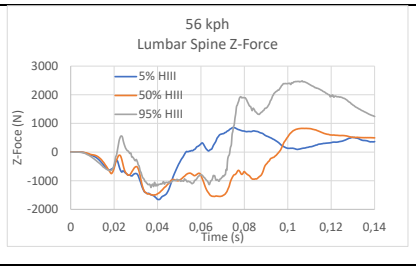	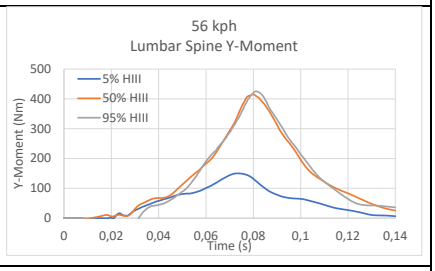
CV	5%HIII:1%, 50%HIII:3%, 95%HIII:1%	5%HIII:4%, 50%HIII:3%, 95%HIII:4%	5%HIII:2%, 50%HIII:2%, 95%HIII:1%

Fig. 12. Average and coefficient of variation lumbar spine x-force, z-force and y-moment

The 5% HIII ATD was not impacting the knee bolster and for the 50% and 95% HIII there was a small knee impact. Therefore, peak compressive forces were low and peak tensile forces ranged from 0.8 for the 5% HIII ATD to 2kN for the 50% HIII ATD (Fig. 13).

CV was excellent for all measurements but for the left femur forces at 40kph impact velocity and right femur forces at 56kph impact velocity for the 95% HIII for which CV was good and acceptable respectively.

	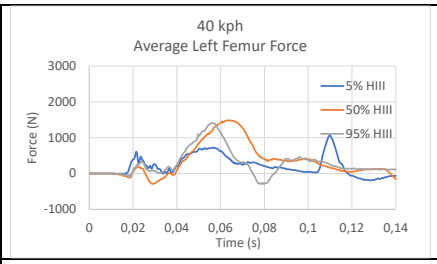	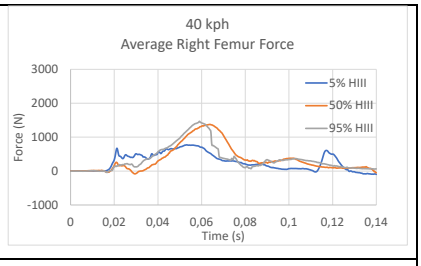
CV	5%HIII:4%, 50%HIII:2%, 95%HIII:7%	5%HIII:2%, 50%HIII:3%, 95%HIII:4%
	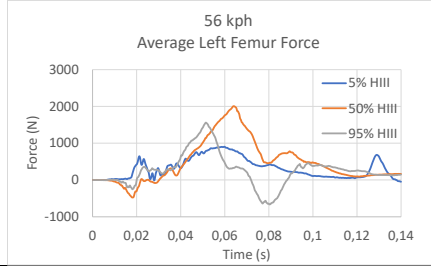	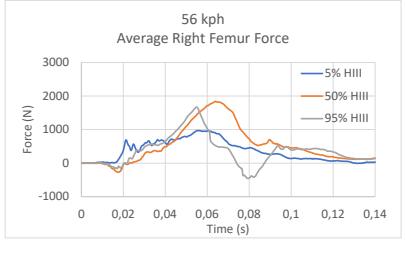
CV	5%HIII:1%, 50%HIII:3%, 95%HIII:5%	5%HIII:1%, 50%HIII:2%, 95%HIII:10%

Fig. 13. Average and coefficient of variation femur left and right force

IV. DISCUSSION

To support validation of the CAE HIII family of ATD models sled tests with the 5%, 50% and 95% HIII dummies in the generic sled test setup was carried out at two different impact velocities. For the assessment of CV a time corridor of 140ms was used for all tests to ensure that all peak values were reached when computing the CV score.Generally, the repeatability of the test results was good. CV for the measurements was excellent with a few exceptions.

Two measurements were classified by CV as unacceptable. These measurements were belt pull in/pull out for the 5% HIII 40kph test, steering column displacement for the 50% HIII 40kph test. For these measurements CV were 26%, 12% respectively. The belt pull in/pull out and steering column displacement measurements were small and close to zero. Despite the high CV the data can be considered useful for model validation due to the fact that the measurements were close to zero and can be considered to be scatter.

A suggested method to position CAE ATD models is to use the H-Point, pelvis angle and belt measurements to position the pelvis and belt. Thereafter use 3D scan data to fine tune the position of the head, upper and lower extremities of the ATD model. In the tests a tolerance of $\pm$10mm for the H-point was considered acceptable. Therefore, a variation of $\pm$10mm in the position of the H-point for the ATD models can be considered reasonable.

The steering column stroke was bottoming out for the 95% HIII ATD in the 56kph tests. No increase in bag pressure due to the bottoming out was observed. However, a second peak in the steering column force due to the bottoming out was observed. Therefore, the steering column force in the 56kph test with the 95% HIII ATD model can be considered not relevant for model validation.

The seat pan stroke barely bottomed out for the 95% HIII in the 56kph test. Therefore, the influence on the test results from the seat pan bottoming out was considered negligible. However, to avoid bottoming out for the 95% HIII in future testing a redesign of the generic seat making the available seat pan stroke longer may be necessary.

In several tests, the seat pan got stuck at peak displacement and did not return to the original position during rebound. However, only small (if any) influence on the test results from the stuck seat pan was observed. Therefore, the influence on the interaction between the ATD and the restraint system was considered negligible.

Other generic validation setups for validation of ATDs in frontal impact comprise a rigid seatpan and no steering column and steering wheel [7]. These boundary conditions are not “vehicle like”. The generic sled model used in this study comprise a semi-rigid seat, a deformable steering column, and an airbag. This makes the generic setup more similar to a vehicle interior than a setup with rigid seat pan, no steering column and steering wheel. Validating the ATD models based on the results from this study results in an evaluation of the ATD with vehicle like yet generic boundary conditions. A validation carried out with these boundary conditions generates more trust that the model will be valid also for analysis of real vehicle interiors than a validation carried out with less vehicle like boundary conditions.

A limitation with the current data set is that the influence of reproducibility not assessed. Therefore, in future testing including different ATDs of the same size can provide an understanding of the influence of reproducibility on the test results.

To enable development of model qualification procedure the results from the testing and a model (LS-DYNA) of the generic frontal impact sled [14] are made available on the openvt.eu platform.

V. CONCLUSION

Sled test results with generally small variability for the 5%, 50% and 95% HIII ATDs were generated in sled tests with clear and thoroughly documented boundary condition making the dataset adequate for development of model certification procedure.

VI. REFERENCES

[1] Klug C., Feist F., et al., "Development of a Certification Procedure for Numerical Pedestrian Models," in: NHTSA (ed.), *The 26th ESV Conference Proceedings*, ESV Conference Proceedings, International Technical Conference on the Enhanced Safety of Vehicles, Eindhoven, Netherlands, 10-13 June:1-24, 2019.

[2] Klug C., Schahner M., et al., "Euro NCAP Virtual Testing – Crashworthiness" *The 27th ESV Conference Proceedings*, ESV Conference Proceedings, International Technical Conference on the Enhanced Safety of Vehicles, Yokohama, Japan, April: 3-26 2023.

[3] EuroNCAP, "Vision 2030, A Safer Future for Mobility", The European New Car Assessment Programme, Belgium, 2022

[4] EuroNCAP, "Assessment Protocol: Adult Occupant Protection", European New Car Assessment Programme, Version 9.2.1., 2022

[5] EuroNCAP, "Virtual Frontal Simulation & Assessment Protocol", Implementation 2026, Version 0.1

[6] Shah C., Khambati S., et al., "Newly Developed LS-DYNA® Models for the THOR-M and Harmonized HIII 50th Crash Test Dummies", *13th International LS-DYNA Users Conference*, Detroit, USA, 2014.

[7] Mohan, P., Park, C-K., et al., *"LSTC/NCAC Dummy Model Development"*, 11th International LS-DYNA Users Conference, Detroit, USA, 2010.

[8] Uriot, J., Potier, P., et al., "Reference PMHS sled tests to Assess Submarining*", Proceedings 59th Stapp Car Crash Conference*, 2015

[9] Mroz K, Östling M, et al., "Effect of Seat and Seat Belt characteristics on the Lumbar Spine and Pelvis Loading of the SAFER Human Body Model in reclined Postures". *Proceedings of the IRCOBI Conference*, 2020, Munich, Germany.

[10] Höschele, P., Smit, S., et al., "Generic Crash Pulses Representing Future Accident Scenarios of Highly 416 Automated Vehicles". SAE International Journal of Transportation Safety, 10(2), doi:10.4271/09-10-02-0010.

[11] HUMANETICS. www.humaneticsgroup.com

[12] Euro NCAP, "Data Format and Injury Criteria Calculation", Technical Bulletin, Version 3.1, June 2020, TB 021, The European New Car Assessment Programme, Belgium

[13] Rhule, D., Rhule, H., Donnelly, B., "The Process of Evaluation and Documentation of Crash Test Dummies for Part 572 of the Code of Federal Regulations." 19th International Technical Conference on the Enhanced Safety of Vehicles, Washington, D.C., USA, 2005.

[14] Valdano, M., Östling, M., Eriksson, L., López-Valdés, F., Pipkorn, B. "Preparing for Virtual Testing for Crashworthiness: Proposing a Method for Certifying ATD Models for Frontal Crash Assessments". *Proceedings of the IRCOBI Conference*, 2024, Stockholm, Sweden.

VII. APPENDIX

Appendix A: Seat, Steering Wheel Measurements

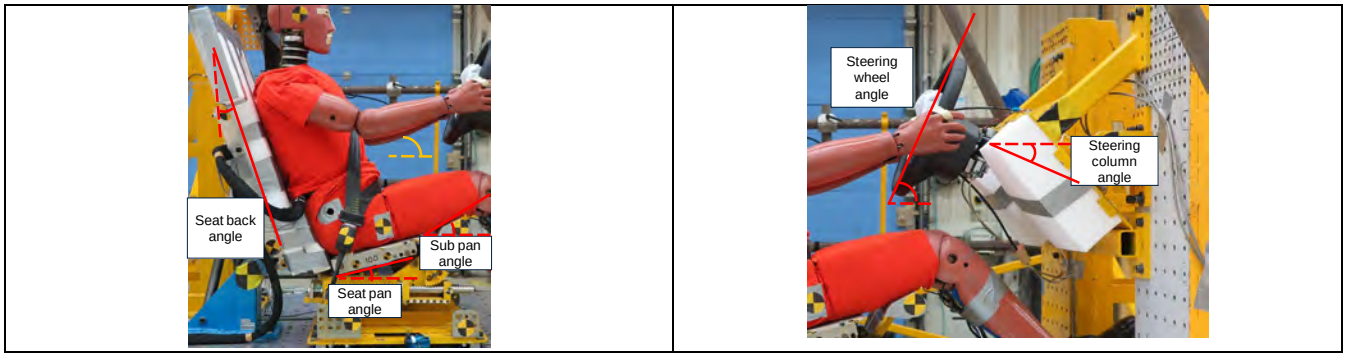

Fig. A1. Seat and Steering Wheel measurements

Table A1. 5% Seat and Steering Wheel Measurements

Test nr:	T-23327671	T-23327672	T-23327673	T-23327674	T-23327675	T-23327676
	40kph	40kph	40kph	56kph	56kph	56kph
Seat back angle (Deg)	20	20	20	20	20	20
Sub pan angle (Deg)	27	27	27	27	27	27
Seat pan angle (Deg)	15	15	15	15	15	15
Steering wheel angle (Deg)	66	66	66	66	66	66
Steering column angle (Deg)	24	24	24	24	24	24

Table A2. 50% Seat and Steering Wheel Measurements

Test nr:	T-23327665	T-23327666	T-23327667	T-23327678	T-23327679	T-23327680
	40kph	40kph	40kph	56kph	56kph	56kph
Seat back angle (Deg)	20	20	20	20	20	20
Sub pan angle (Deg)	26	26	26	26	26	25
Seat pan angle (Deg)	15	15	15	15	15	15
Steering wheel angle (Deg)	66	66	66	66	66	66
Steering column angle (Deg)	26	26	26	26	26	26

Table A3. 95% Seat and Steering Wheel Measurements

Test nr:	T-23327677	T-23327678	T-23327679	T-23327680	T-23327681	T-23327682
	40kph	40kph	40kph	56kph	56kph	56kph
Seat back angle (Deg)	19	19	19	19	19	19
Sub pan angle (Deg)	27	27	27	27	28	27
Seat pan angle (Deg)	15	15	15	15	15	15
Steering wheel angle (Deg)	65	65	65	65	65	65
Steering column angle (Deg)	25	25	25	25	25	25

Appendix B: Sled Transducer Type and Manufacturer

Table B1. Transducer Type and Manufacturer

Sensor type	Sensor ID	Manufacturer	Model
Sled acc. X-dir.	A1X-301	Entran	EGCS-D1M-100
Steering column force LH	KR5-006	Load Indicator AB	PA5
Steering column force RH	KR5-007	Load Indicator AB	PA5
Lower neck forward disp.	LG-130	SpaceAge	162-2945-C8SS999
Seat pan disp.	LG-145	SpaceAge	160-1615-C8SU9
Seat Belt at Retractor Disp.	LG-200E	IES	IES-2098
Airbag inflator pressure	TR-231	Endevco	8510C-100 M37
Pelvis forward disp.	LG-115	SpaceAge	160-1615-C8SU9
Seat Belt Load at Retractor	BK-087	Messring	5BCD1622
Seat Belt Load at Upper Diagonal Belt	BK-069	Messring	DK11-35-23
Seat Belt Load at Lap Belt Outside	BK-075	Messring	DK11-35-23
Airbag cushion pressure	TR-233	Endevco	8510C-100 M37
Steering column disp.	LG-113	SpaceAge	160-1615-C8SU9
Sled Trigg acc.	A1X-312	Entran	EGCS-D1M-100

Appendix C: Target Coordinates with Tolerances and Measurements

Table C1. 5% HIII Target Coordinates with Tolerances

Test nr:							T-23327671			T-23327672			T-23327673			T-23327674			T-23327675			T-23327676		
							40kph			40kph			40kph			56kph			56kph			56kph		
	Target			Tolerance																				
	x	y	z	x	y	z	x	y	z	x	y	z	x	y	z	x	y	z	x	y	z	x	y	z
H-Point (mm)	-120		-169	±10		±10	-120		-169	-120		-169	-120		-167	-120		-166	-120		-166	-120		-166
Head Angle (Deg)		0			+1			0			0			0			0			0			0	
Pelvis Angle (Deg)		20		+1				21			19			20			21			20			21	
Femur Angles LH/RH (Deg)		12						13/12			12/13			13/12			13/11			13/13			12/12	
Tibia Angles LH/RH (Deg)		-50						-51/-52			-52/-51			-51/-51			-53/-51			-52/-51			-52/-51	

Table C2. 50% HIII Target Coordinates with Tolerances

Test nr:							T-23327665			T-23327666			T-23327667			T-23327678			T-23327679			T-23327680		
							40kph			40kph			40kph			56kph			56kph			56kph		
	Target			Tolerance																				
	x	y	z	x	y	z	x	y	z	x	y	z	x	y	z	x	y	z	x	y	z	x	y	z
H-Point (mm)	-103		-162	±10		±10	-103		-159	-103		-160	-103		-160	-103		-159	-103		-158	-103		-158
Head Angle (Deg)		0			+1			0			0			0			0			0			0	
Pelvis Angle (Deg)		23		+1				22			21			21			22			21			22	
Femur Angles LH/RH (Deg)		213						13/16			14/18			12/15			12/15			12/15			11/15	
Tibia Angles LH/RH (Deg)		-60						-48/-49			-49/-50			-46/-49			-47/-49			-46/-48			-45/-48	

Table C3. 95% HIII Target Coordinates with Tolerances

Test nr:							T-23327677			T-23327678			T-23327679			T-23327680			T-23327681			T-23327682		
							40kph			40kph			40kph			56kph			56kph			56kph		
	Target			Tolerance																				
	x	y	z	x	y	z	x	y	z	x	y	z	x	y	z	x	y	z	x	y	z	x	y	z
H-Point (mm)	-108		-168	±10		±10	-108		-167	-108		-168	-108		-167	-108		-168	-108		-167	-108		-170
Head Angle (Deg)		0			+1			0			0			0			0			0			0	
Pelvis Angle (Deg)		23		+1				21			20			20			21			21			22	
Femur Angles LH/RH (Deg)		15						15/16			15/16			16/16			15/15			15/16			16/15	
Tibia Angles LH/RH (Deg)		-53						-54/-53			-53/-53			-53/53			-53/52			-54/-54			-54/-53	

Appendix D: Nose to Upper Rim and Belt Measurements

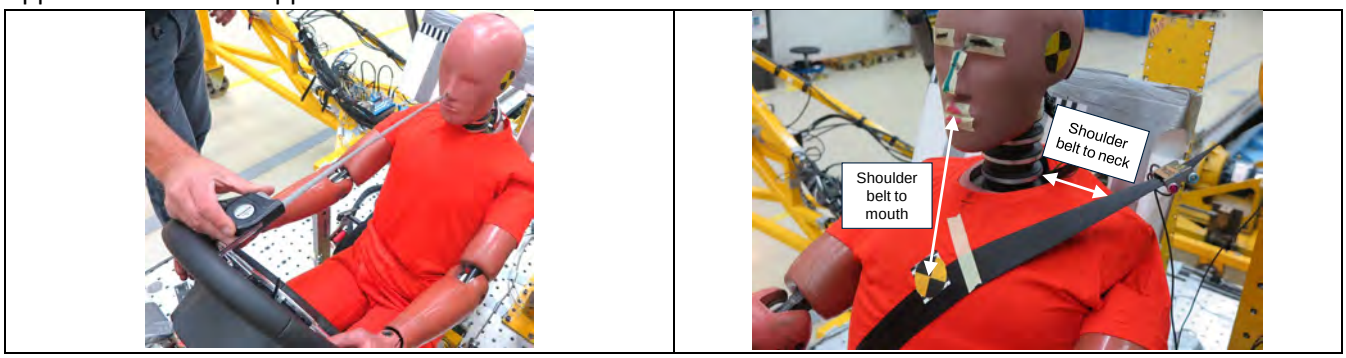

Fig. D1. Nose to Rim, Shoulder belt to Mouth and Shoulder Belt to Neck Measurements

Table D1. 5% Shoulder belt to Mouth and Shoulder Belt to Neck Measurements

Test nr:	T-23327671	T-23327672	T-23327673	T-23327674	T-23327675	T-23327676
	40kph	40kph	40kph	56kph	56kph	56kph
Nose to upper rim	382	382	382	382	382	382
Belt to neck	53	47	51	49	51	51
Belt to mouth	160	160	160	160	160	160

Table D2. 50% Shoulder belt to Mouth and Shoulder Belt to Neck Measurements

Test nr:	T-23327665	T-23327666	T-23327667	T-23327678	T-23327679	T-23327680
	40kph	40kph	40kph	56kph	56kph	56kph
Nose to upper rim	490	490	490	490	490	490
Belt to neck	67	67	70	66	68	66
Belt to mouth	175	175	175	175	175	175

Table D3. 95% Shoulder belt to Mouth and Shoulder Belt to Neck Measurements

Test nr:	T-23327677	T-23327678	T-23327679	T-23327680	T-23327681	T-23327682
	40kph	40kph	40kph	56kph	56kph	56kph
Nose to upper rim	**250**	**250**	**250**	**250**	**250**	**250**
Belt to neck	485	485	485	485	485	485
Belt to mouth	200	200	200	200	200	200

Appendix E: 5% HIII Dummy Results

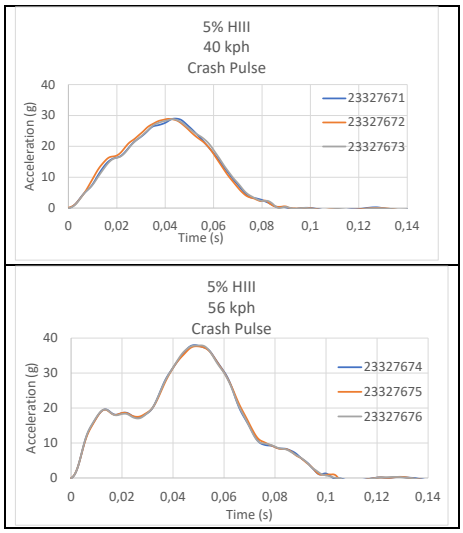

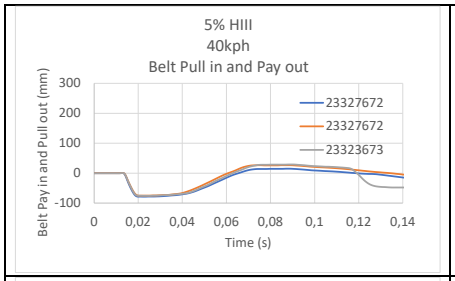

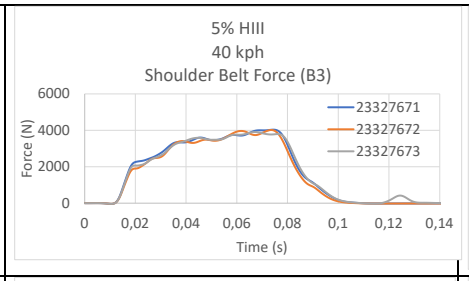

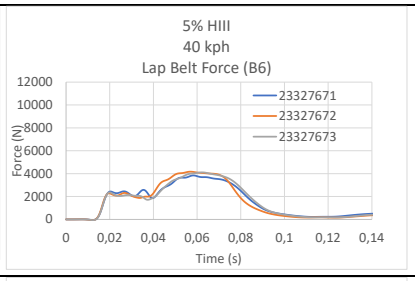

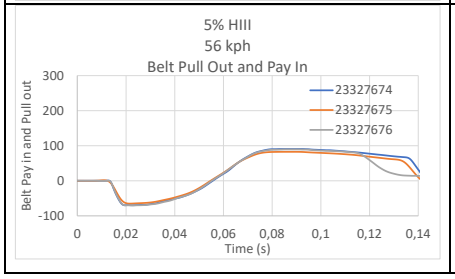

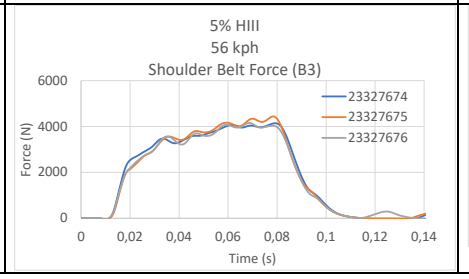

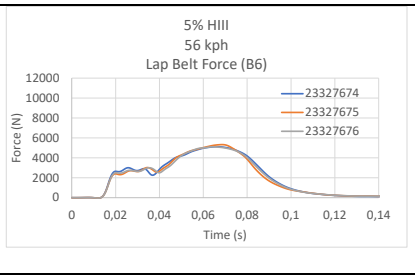

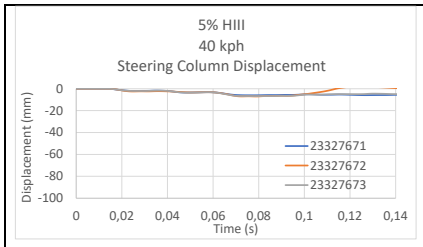

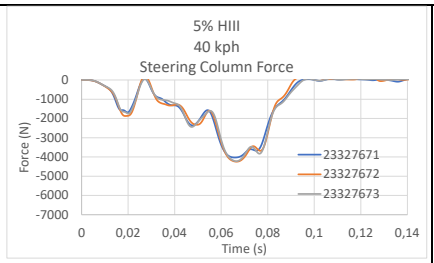

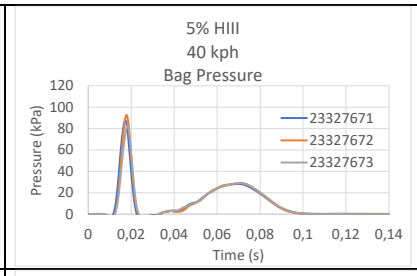

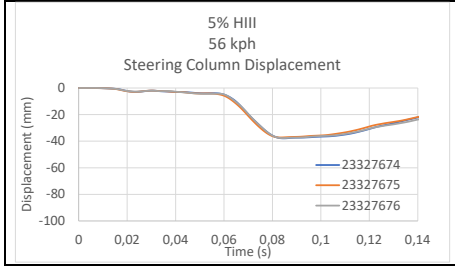

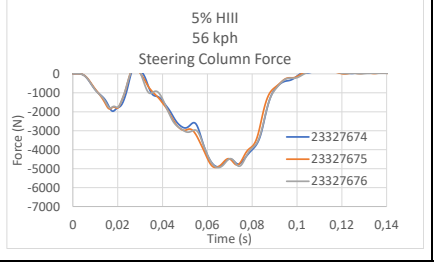

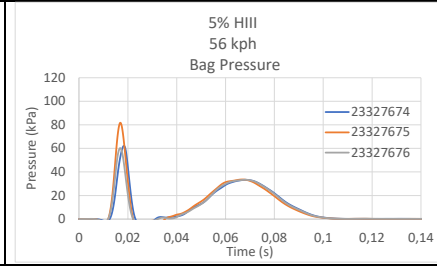

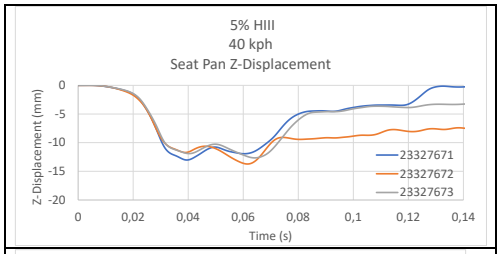
5% HIII
40 kph
Seat Pan Z-Displacement
Z-Displacement (mm)
Time (s)
23327671
23327672
23327673

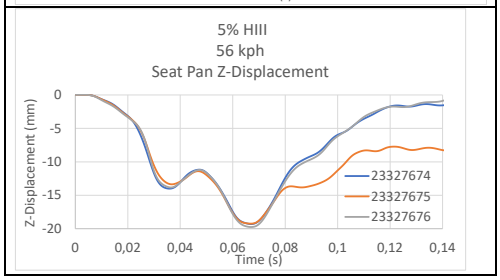
5% HIII
56 kph
Seat Pan Z-Displacement
Z-Displacement (mm)
Time (s)
23327674
23327675
23327676

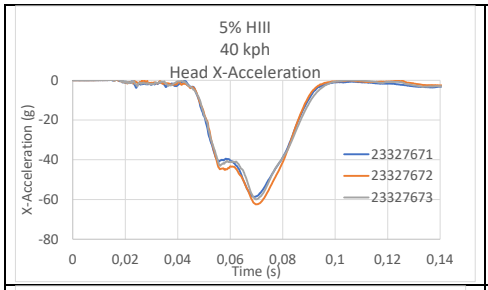
5% HIII
40 kph
Head X-Acceleration
X-Acceleration (g)
Time (s)
23327671
23327672
23327673

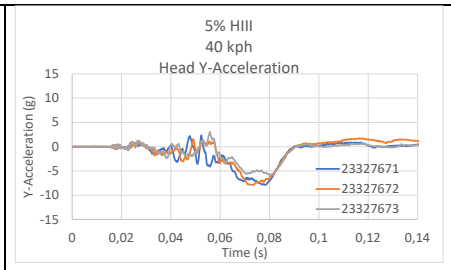
5% HIII
40 kph
Head Y-Acceleration
Y-Acceleration (g)
Time (s)
23327671
23327672
23327673

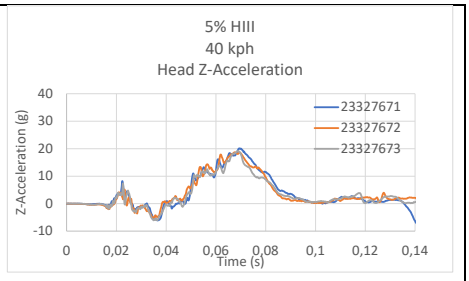
5% HIII
40 kph
Head Z-Acceleration
Z-Acceleration (g)
Time (s)
23327671
23327672
23327673

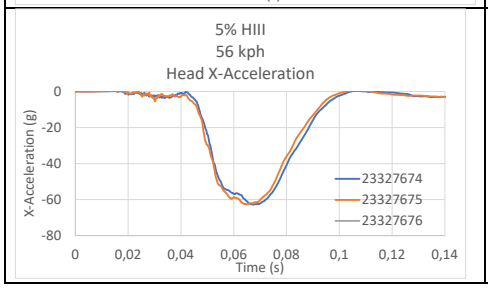
5% HIII
56 kph
Head X-Acceleration
X-Acceleration (g)
Time (s)
23327674
23327675
23327676

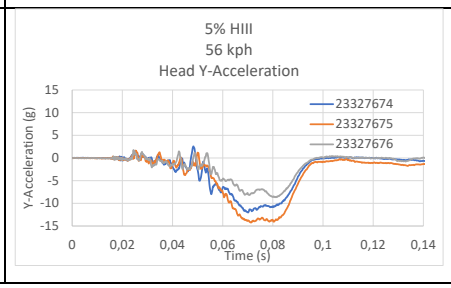
5% HIII
56 kph
Head Y-Acceleration
Y-Acceleration (g)
Time (s)
23327674
23327675
23327676

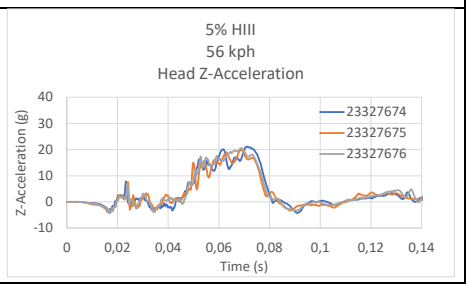
5% HIII
56 kph
Head Z-Acceleration
Z-Acceleration (g)
Time (s)
23327674
23327675
23327676

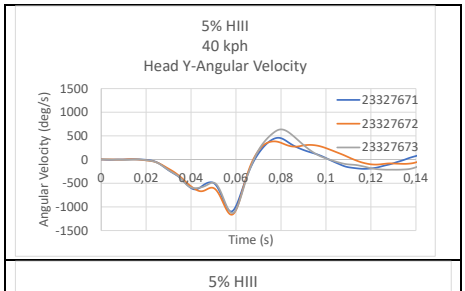
5% HIII
40 kph
Head Y-Angular Velocity
Angular Velocity (deg/s)
Time (s)
23327671
23327672
23327673

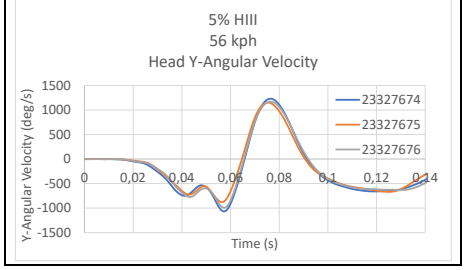
5% HIII
56 kph
Head Y-Angular Velocity
Y-Angular Velocity (deg/s)
Time (s)
23327674
23327675
23327676

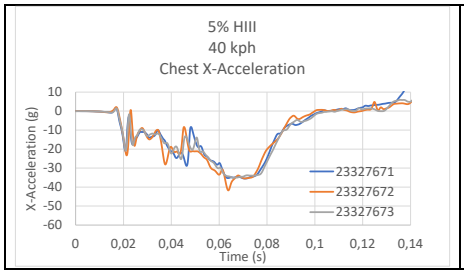
5% HIII
40 kph
Chest X-Acceleration
X-Acceleration (g)
Time (s)
23327671
23327672
23327673

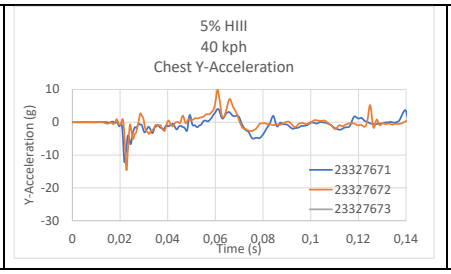
5% HIII
40 kph
Chest Y-Acceleration
Y-Acceleration (g)
Time (s)
23327671
23327672
23327673

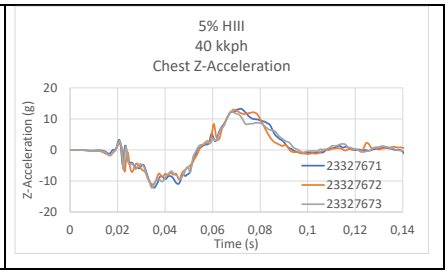
5% HIII
40 kkph
Chest Z-Acceleration
Z-Acceleration (g)
Time (s)
23327671
23327672
23327673

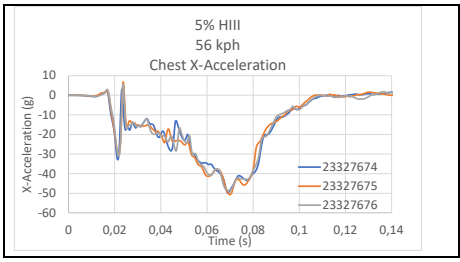
5% HIII
56 kph
Chest X-Acceleration
X-Acceleration (g)
Time (s)
23327674
23327675
23327676

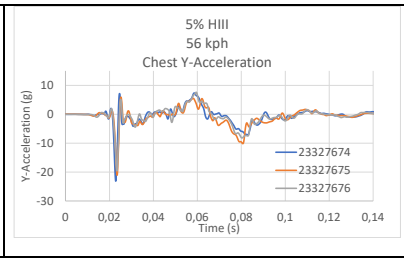
5% HIII
56 kph
Chest Y-Acceleration
Y-Acceleration (g)
Time (s)
23327674
23327675
23327676

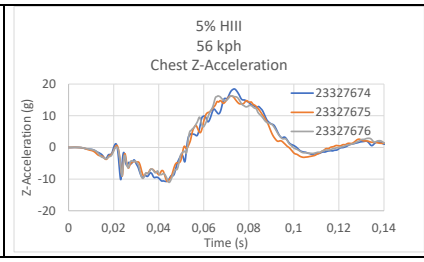
5% HIII
56 kph
Chest Z-Acceleration
Z-Acceleration (g)
Time (s)
23327674
23327675
23327676

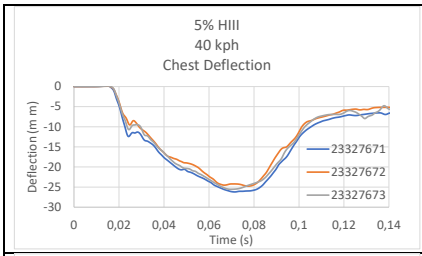
5% HIII
40 kph
Chest Deflection
Deflection (m m)
Time (s)
23327671
23327672
23327673

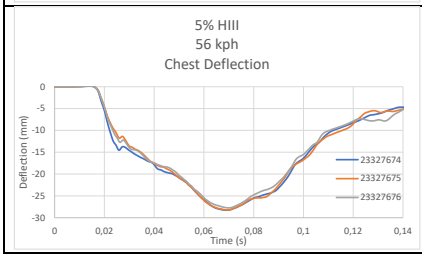
5% HIII
56 kph
Chest Deflection
Deflection (mm)
Time (s)
23327674
23327675
23327676

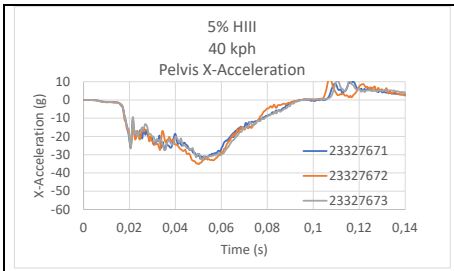
5% HIII
40 kph
Pelvis X-Acceleration
X-Acceleration (g)
Time (s)
23327671
23327672
23327673

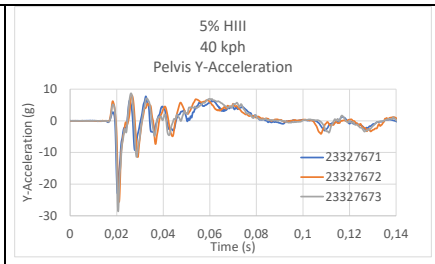
5% HIII
40 kph
Pelvis Y-Acceleration
Y-Acceleration (g)
Time (s)
23327671
23327672
23327673

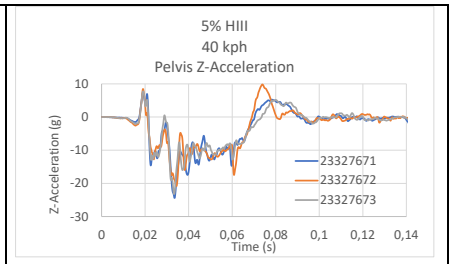
5% HIII
40 kph
Pelvis Z-Acceleration
Z-Acceleration (g)
Time (s)
23327671
23327672
23327673

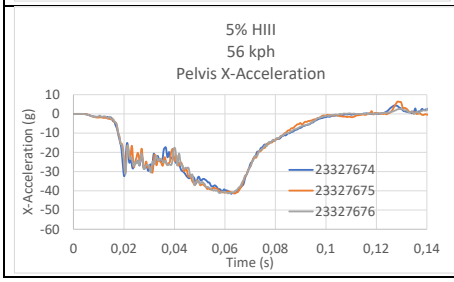
5% HIII
56 kph
Pelvis X-Acceleration
X-Acceleration (g)
Time (s)
23327674
23327675
23327676

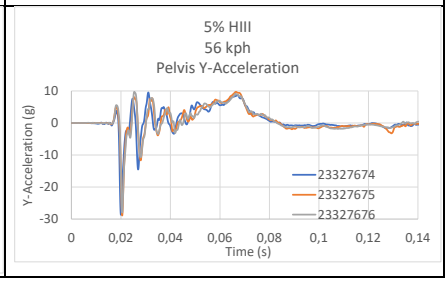
5% HIII
56 kph
Pelvis Y-Acceleration
Y-Acceleration (g)
Time (s)
23327674
23327675
23327676

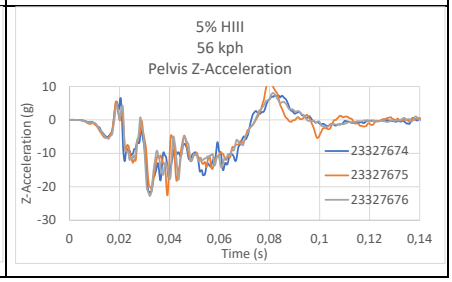
5% HIII
56 kph
Pelvis Z-Acceleration
Z-Acceleration (g)
Time (s)
23327674
23327675
23327676

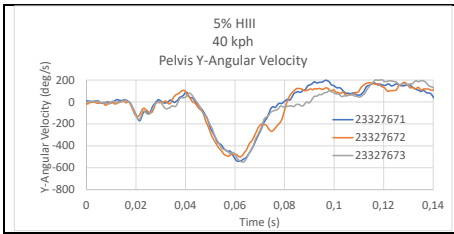
5% HIII
40 kph
Pelvis Y-Angular Velocity
Y-Angular Velocity (deg/s)
Time (s)
23327671
23327672
23327673

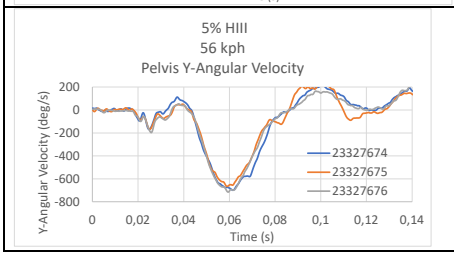
5% HIII
56 kph
Pelvis Y-Angular Velocity
Y-Angular Velocity (deg/s)
Time (s)
23327674
23327675
23327676

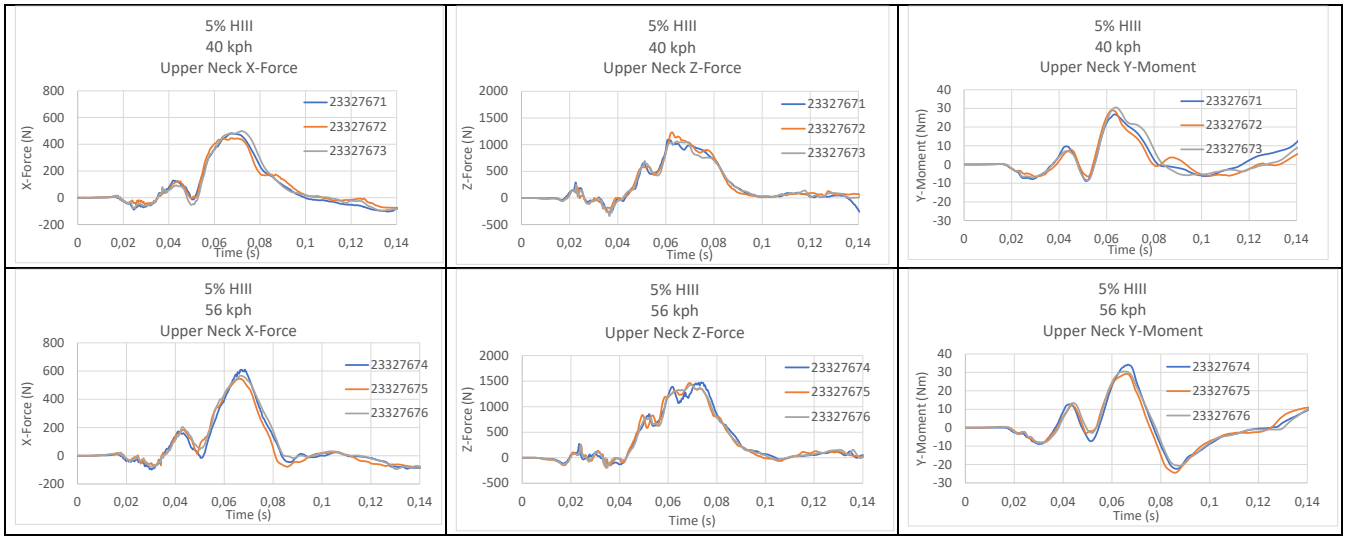
5% HIII
40 kph
Upper Neck X-Force
X-Force (N)
Time (s)
23327671
23327672
23327673
5% HIII
40 kph
Upper Neck Z-Force
Z-Force (N)
Time (s)
23327671
23327672
23327673
5% HIII
40 kph
Upper Neck Y-Moment
Y-Moment (Nm)
Time (s)
23327671
23327672
23327673
5% HIII
56 kph
Upper Neck X-Force
X-Force (N)
Time (s)
23327674
23327675
23327676
5% HIII
56 kph
Upper Neck Z-Force
Z-Force (N)
Time (s)
23327674
23327675
23327676
5% HIII
56 kph
Upper Neck Y-Moment
Y-Moment (Nm)
Time (s)
23327674
23327675
23327676

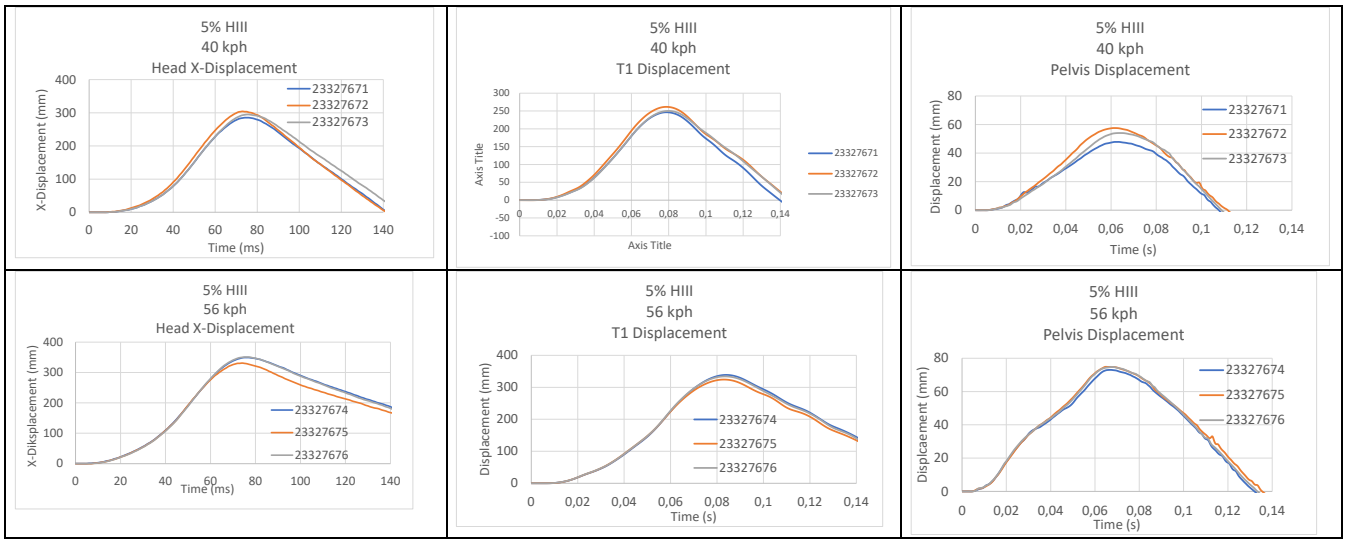
5% HIII
40 kph
Head X-Displacement
X-Displacement (mm)
Time (ms)
23327671
23327672
23327673
5% HIII
40 kph
T1 Displacement
Axis Title
Axis Title
23327671
23327672
23327673
5% HIII
40 kph
Pelvis Displacement
Displacement (mm)
Time (s)
23327671
23327672
23327673
5% HIII
56 kph
Head X-Displacement
X-Diksplacement (mm)
Time (ms)
23327674
23327675
23327676
5% HIII
56 kph
T1 Displacement
Displacement (mm)
Time (s)
23327674
23327675
23327676
5% HIII
56 kph
Pelvis Displacement
Displcaement (mm)
Time (s)
23327674
23327675
23327676

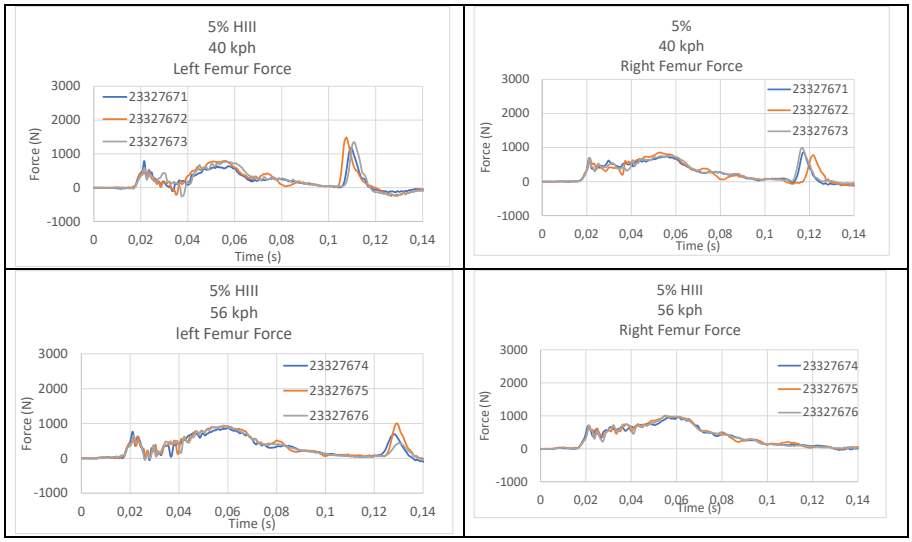
5% HIII
40 kph
Left Femur Force
Force (N)
Time (s)
23327671
23327672
23327673
5%
40 kph
Right Femur Force
Force (N)
Time (s)
23327671
23327672
23327673
5% HIII
56 kph
left Femur Force
Force (N)
Time (s)
23327674
23327675
23327676
5% HIII
56 kph
Right Femur Force
Force (N)
Time (s)
23327674
23327675
23327676

APPENDIX F: 50% HIII Dummy Results

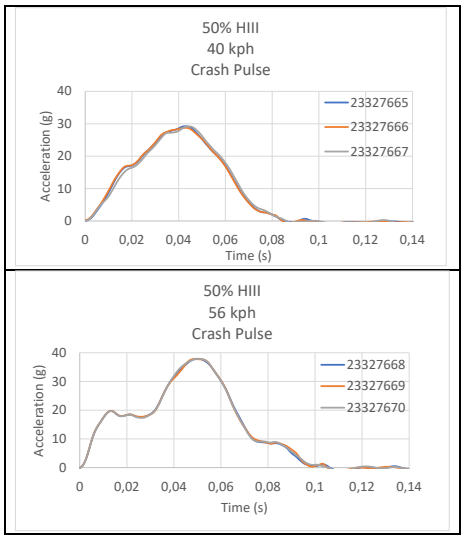

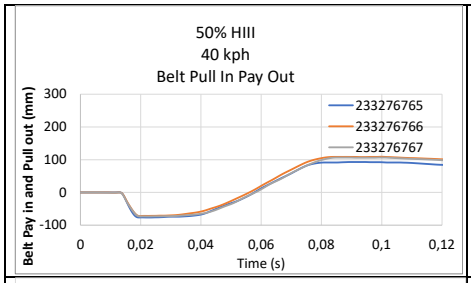

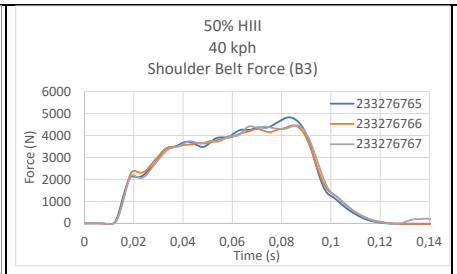

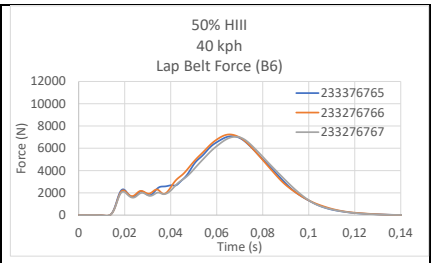

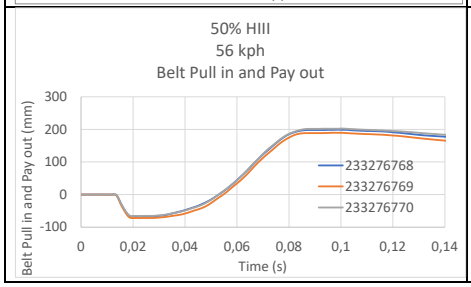

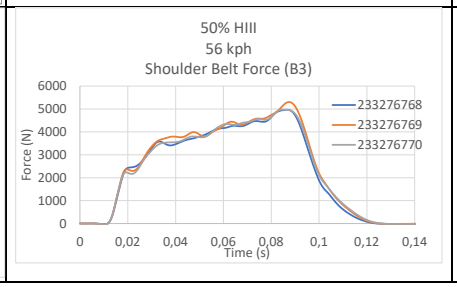

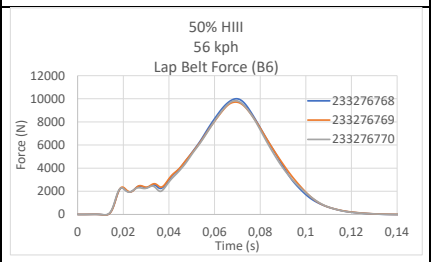

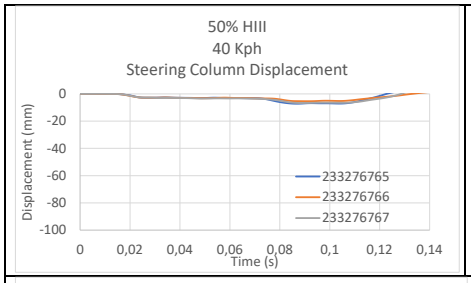

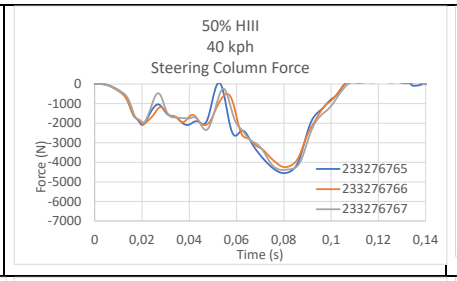

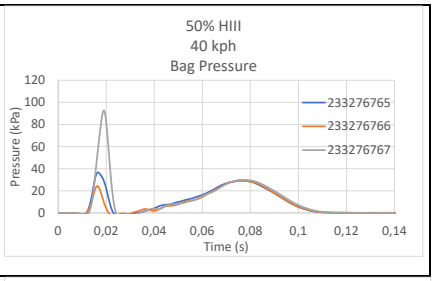

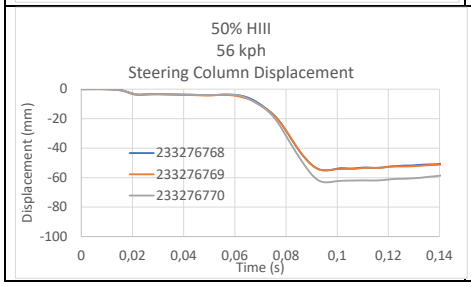

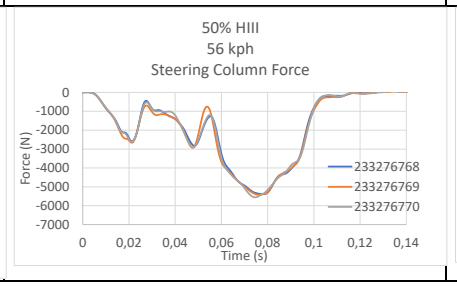

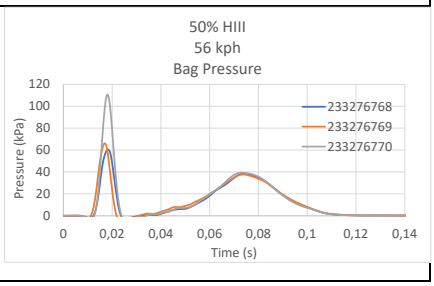

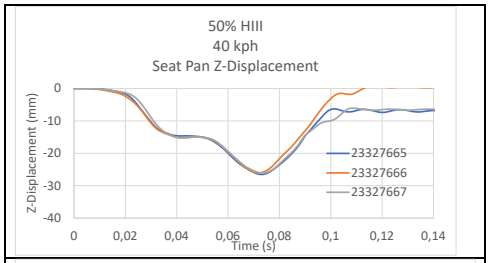
50% HIII
40 kph
Seat Pan Z-Displacement
Z-Displacement (mm)
Time (s)
23327665
23327666
23327667

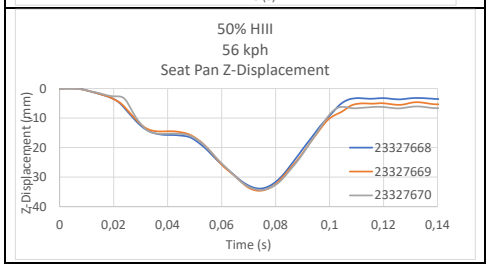
50% HIII
56 kph
Seat Pan Z-Displacement
Z-Displacement (mm)
Time (s)
23327668
23327669
23327670

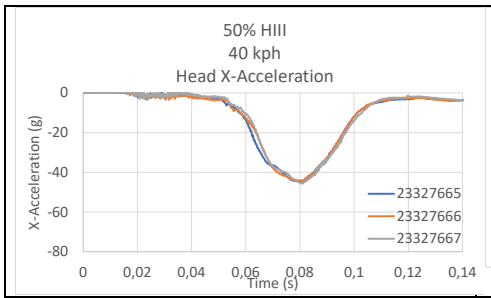
50% HIII
40 kph
Head X-Acceleration
X-Acceleration (g)
Time (s)
23327665
23327666
23327667

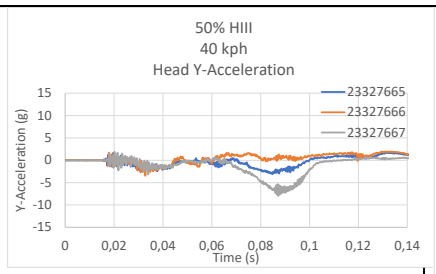
50% HIII
40 kph
Head Y-Acceleration
Y-Acceleration (g)
Time (s)
23327665
23327666
23327667

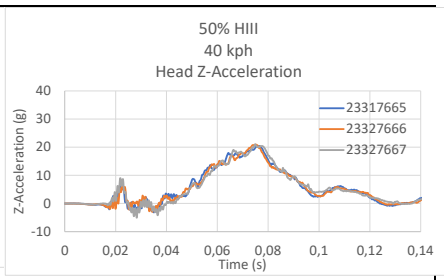
50% HIII
40 kph
Head Z-Acceleration
Z-Acceleration (g)
Time (s)
23317665
23327666
23327667

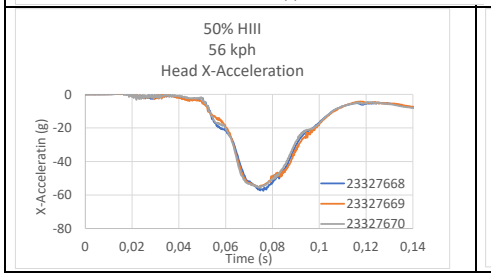
50% HIII
56 kph
Head X-Acceleration
X-Acceleratin (g)
Time (s)
23327668
23327669
23327670

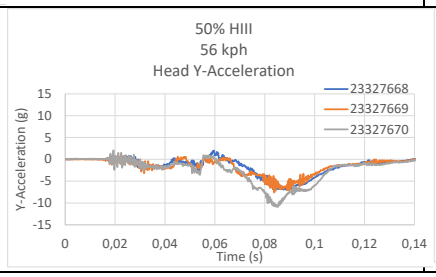
50% HIII
56 kph
Head Y-Acceleration
Y-Acceleration (g)
Time (s)
23327668
23327669
23327670

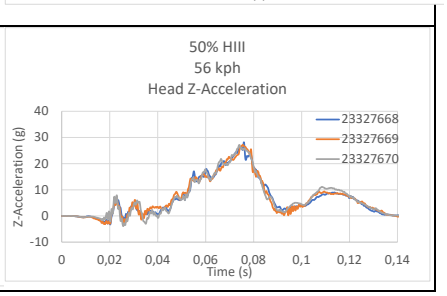
50% HIII
56 kph
Head Z-Acceleration
Z-Acceleration (g)
Time (s)
23327668
23327669
23327670

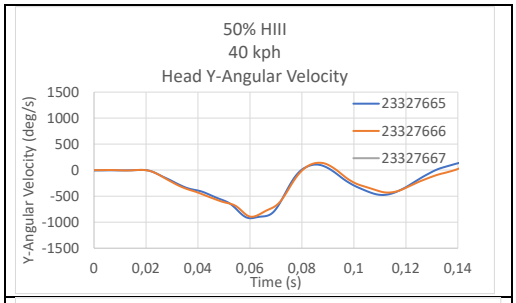
50% HIII
40 kph
Head Y-Angular Velocity
Y-Angular Velocity (deg/s)
Time (s)
23327665
23327666
23327667

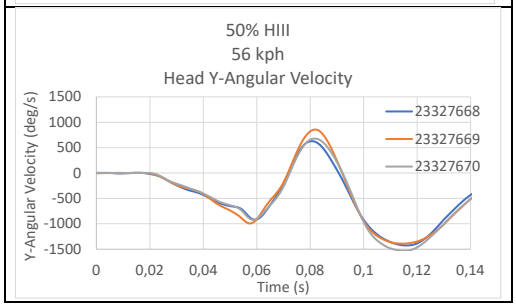
50% HIII
56 kph
Head Y-Angular Velocity
Y-Angular Velocity (deg/s)
Time (s)
23327668
23327669
23327670

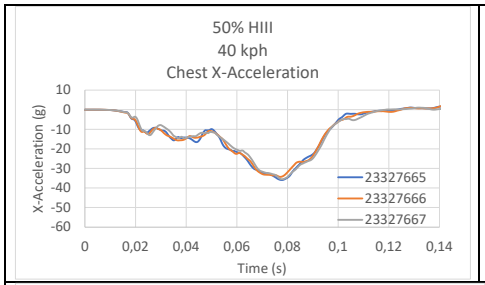
50% HIII
40 kph
Chest X-Acceleration
X-Acceleration (g)
Time (s)
23327665
23327666
23327667

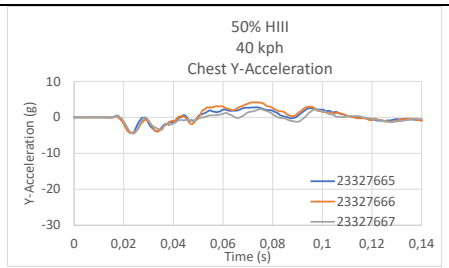
50% HIII
40 kph
Chest Y-Acceleration
Y-Acceleration (g)
Time (s)
23327665
23327666
23327667

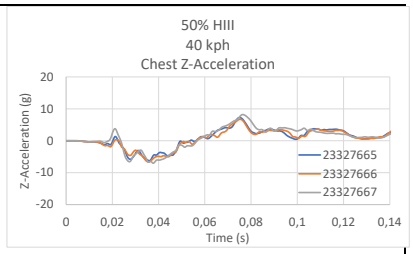
50% HIII
40 kph
Chest Z-Acceleration
Z-Acceleration (g)
Time (s)
23327665
23327666
23327667

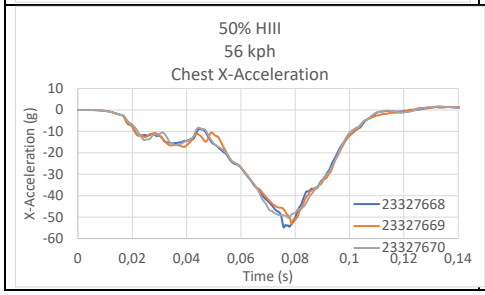
50% HIII
56 kph
Chest X-Acceleration
X-Acceleration (g)
Time (s)
23327668
23327669
23327670

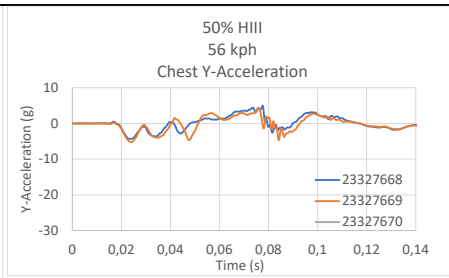
50% HIII
56 kph
Chest Y-Acceleration
Y-Acceleration (g)
Time (s)
23327668
23327669
23327670

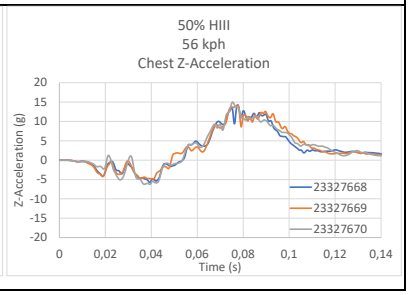
50% HIII
56 kph
Chest Z-Acceleration
Z-Acceleration (g)
Time (s)
23327668
23327669
23327670

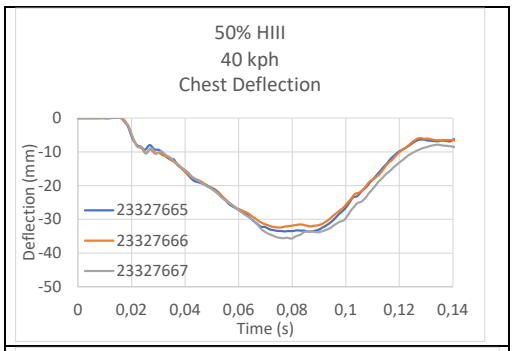
50% HIII
40 kph
Chest Deflection
Deflection (mm)
Time (s)
23327665
23327666
23327667

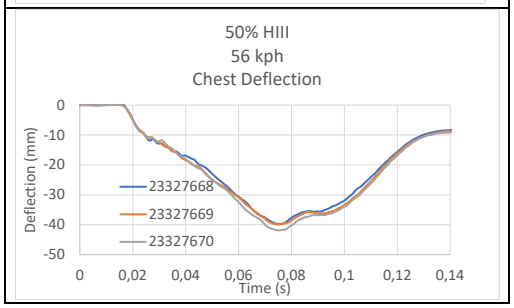
50% HIII
56 kph
Chest Deflection
Deflection (mm)
Time (s)
23327668
23327669
23327670

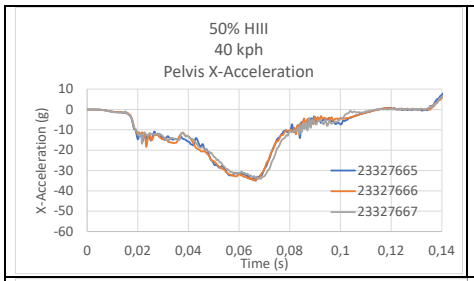
50% HIII
40 kph
Pelvis X-Acceleration
X-Acceleration (g)
Time (s)
23327665
23327666
23327667

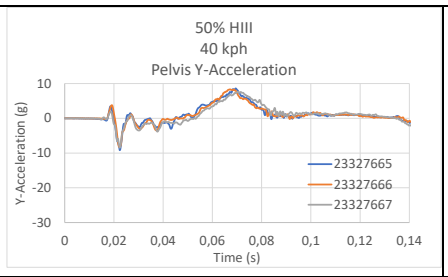
50% HIII
40 kph
Pelvis Y-Acceleration
Y-Acceleration (g)
Time (s)
23327665
23327666
23327667

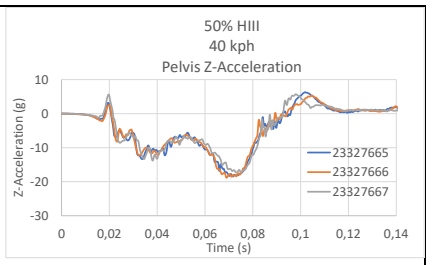
50% HIII
40 kph
Pelvis Z-Acceleration
Z-Acceleration (g)
Time (s)
23327665
23327666
23327667

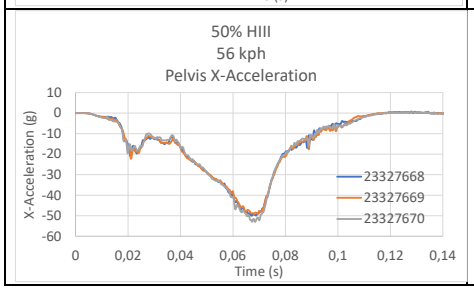
50% HIII
56 kph
Pelvis X-Acceleration
X-Acceleration (g)
Time (s)
23327668
23327669
23327670

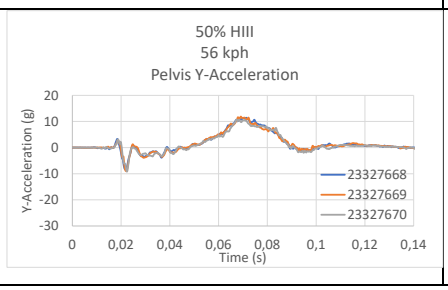
50% HIII
56 kph
Pelvis Y-Acceleration
Y-Acceleration (g)
Time (s)
23327668
23327669
23327670

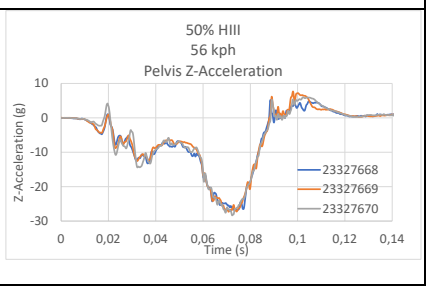
50% HIII
56 kph
Pelvis Z-Acceleration
Z-Acceleration (g)
Time (s)
23327668
23327669
23327670

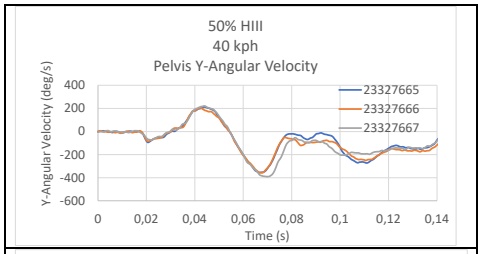
50% HIII
40 kph
Pelvis Y-Angular Velocity
Y-Angular Velocity (deg/s)
Time (s)
23327665
23327666
23327667

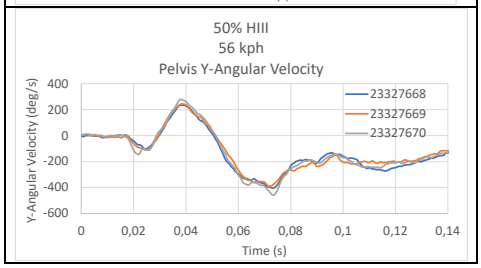
50% HIII
56 kph
Pelvis Y-Angular Velocity
Y-Angular Velocity (deg/s)
Time (s)
23327668
23327669
23327670

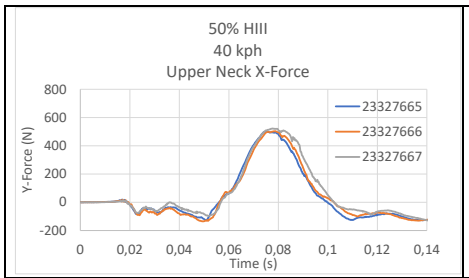
50% HIII
40 kph
Upper Neck X-Force
Y-Force (N)
Time (s)
23327665
23327666
23327667

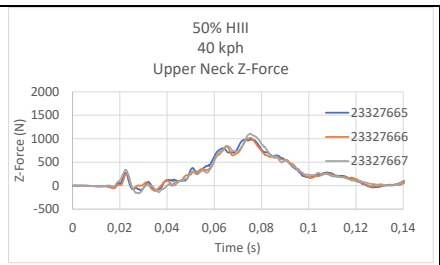
50% HIII
40 kph
Upper Neck Z-Force
Z-Force (N)
Time (s)
23327665
23327666
23327667

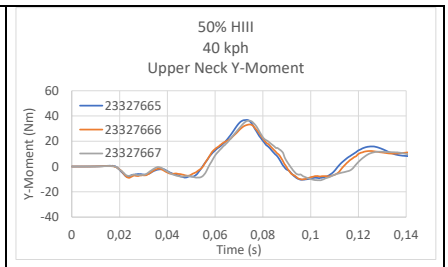
50% HIII
40 kph
Upper Neck Y-Moment
Y-Moment (Nm)
Time (s)
23327665
23327666
23327667

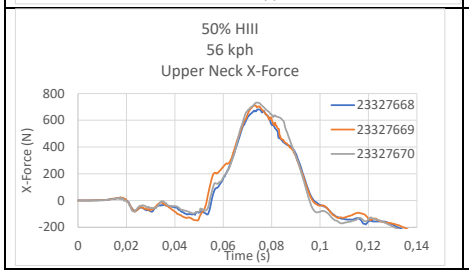
50% HIII
56 kph
Upper Neck X-Force
X-Force (N)
Time (s)
23327668
23327669
23327670

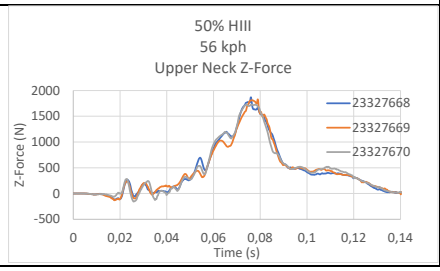
50% HIII
56 kph
Upper Neck Z-Force
Z-Force (N)
Time (s)
23327668
23327669
23327670

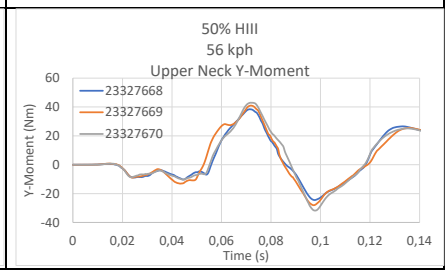
50% HIII
56 kph
Upper Neck Y-Moment
Y-Moment (Nm)
Time (s)
23327668
23327669
23327670

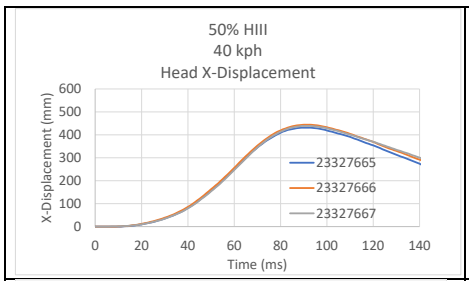
50% HIII
40 kph
Head X-Displacement
X-Displacement (mm)
Time (ms)
23327665
23327666
23327667

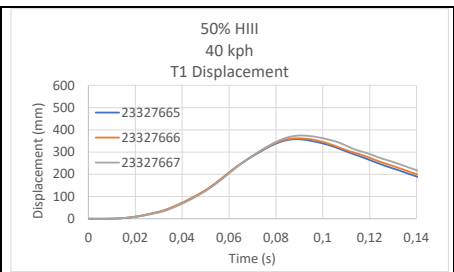
50% HIII
40 kph
T1 Displacement
Displacement (mm)
Time (s)
23327665
23327666
23327667

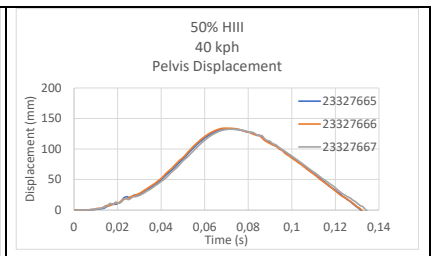
50% HIII
40 kph
Pelvis Displacement
Displacement (mm)
Time (s)
23327665
23327666
23327667

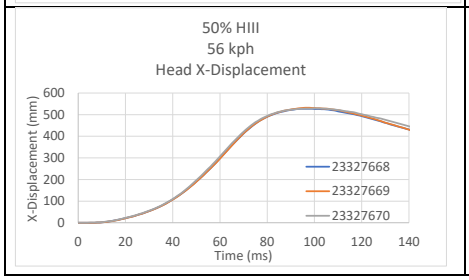
50% HIII
56 kph
Head X-Displacement
X-Displacement (mm)
Time (ms)
23327668
23327669
23327670

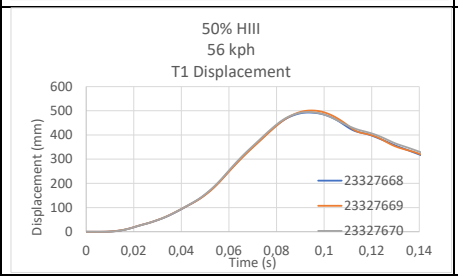
50% HIII
56 kph
T1 Displacement
Displacement (mm)
Time (s)
23327668
23327669
23327670

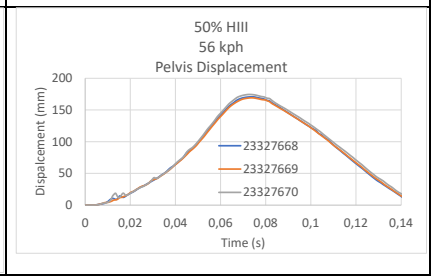
50% HIII
56 kph
Pelvis Displacement
Displacement (mm)
Time (s)
23327668
23327669
23327670

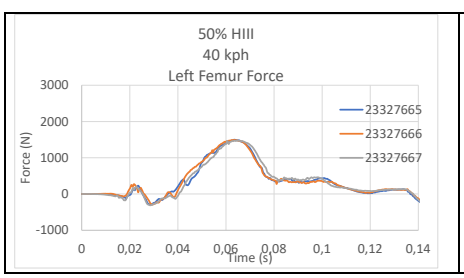
50% HIII
40 kph
Left Femur Force
Force (N)
Time (s)
23327665
23327666
23327667

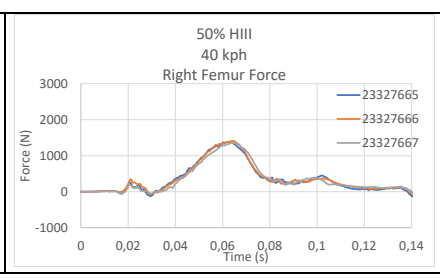
50% HIII
40 kph
Right Femur Force
Force (N)
Time (s)
23327665
23327666
23327667

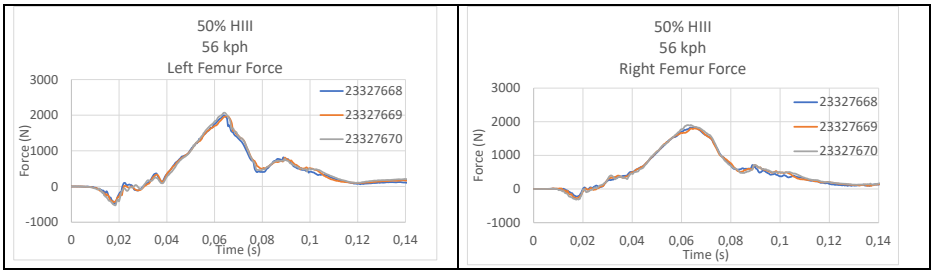
50% HIII
56 kph
Left Femur Force
Force (N)
Time (s)
23327668
23327669
23327670
50% HIII
56 kph
Right Femur Force
Force (N)
Time (s)
23327668
23327669
23327670

APPENDIX G: 95% HIII Dummy Results

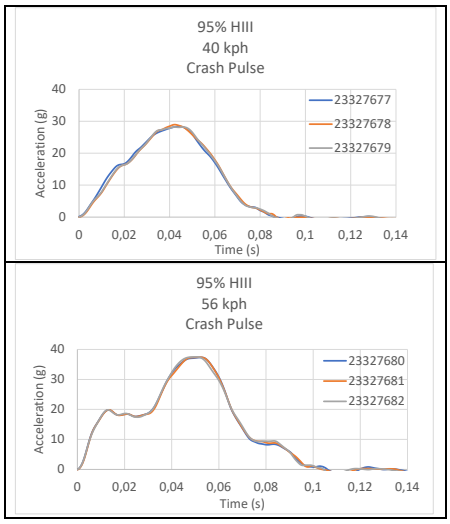

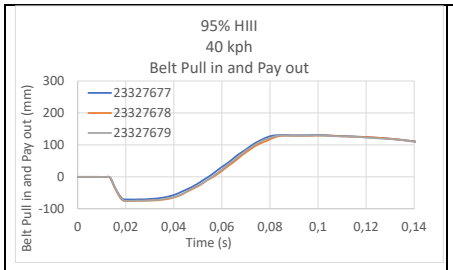

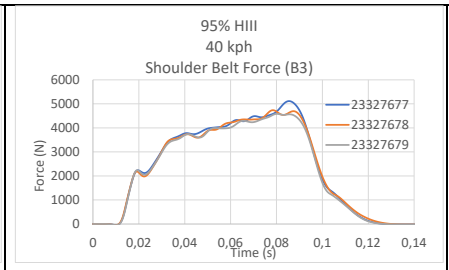

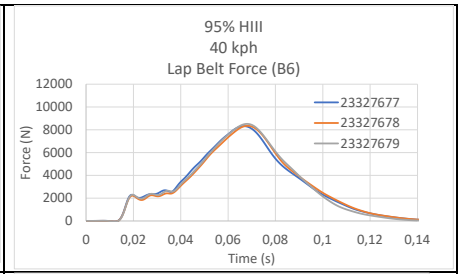

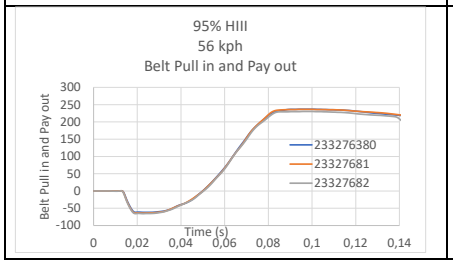

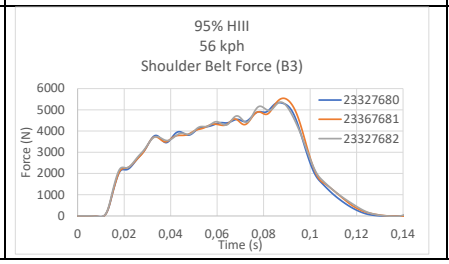

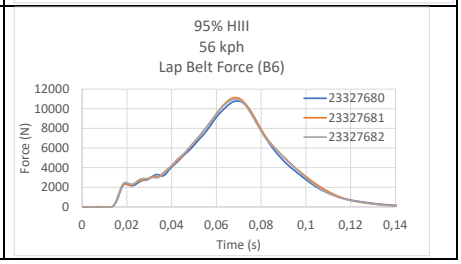

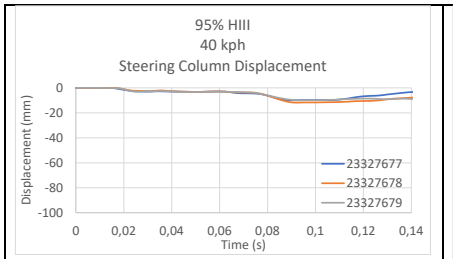

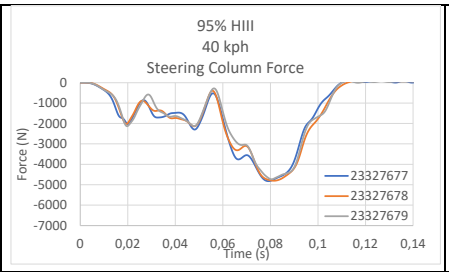

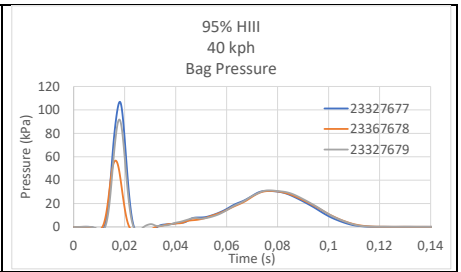

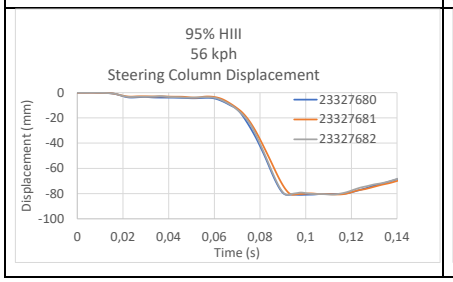

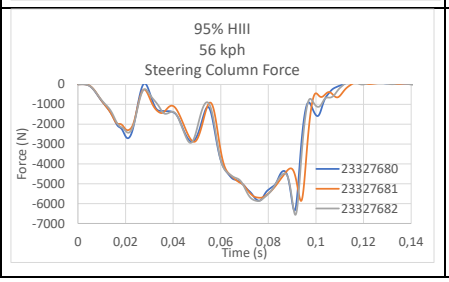

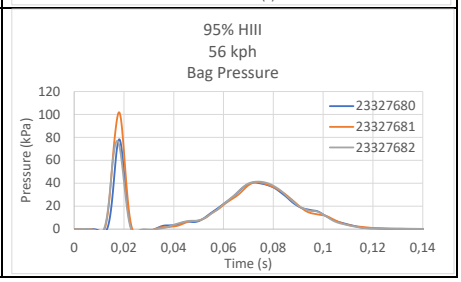

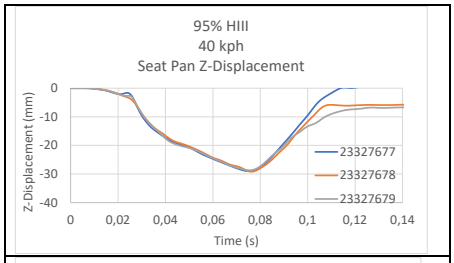
95% HIII
40 kph
Seat Pan Z-Displacement
Z-Displacement (mm)
Time (s)
23327677
23327678
23327679

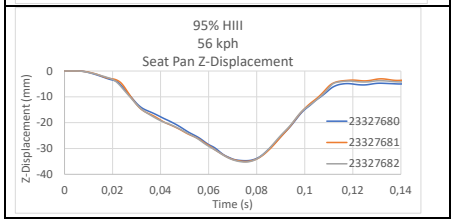
95% HIII
56 kph
Seat Pan Z-Displacement
Z-Displacement (mm)
Time (s)
23327680
23327681
23327682

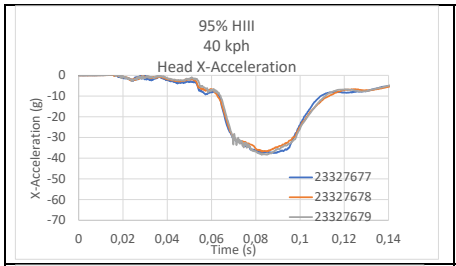
95% HIII
40 kph
Head X-Acceleration
X-Acceleration (g)
Time (s)
23327677
23327678
23327679

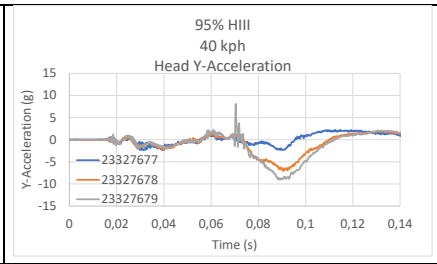
95% HIII
40 kph
Head Y-Acceleration
Y-Acceleration (g)
Time (s)
23327677
23327678
23327679

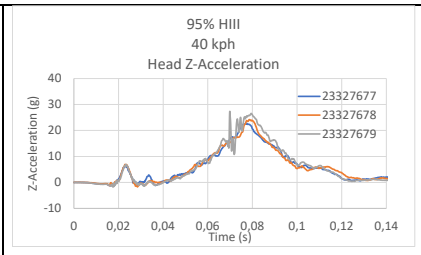
95% HIII
40 kph
Head Z-Acceleration
Z-Acceleration (g)
Time (s)
23327677
23327678
23327679

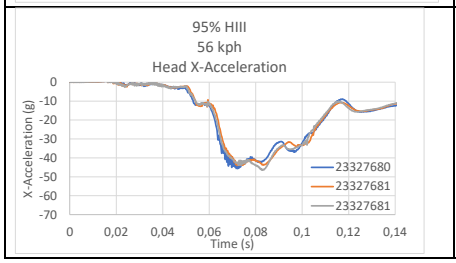
95% HIII
56 kph
Head X-Acceleration
X-Acceleration (g)
Time (s)
23327680
23327681
23327681

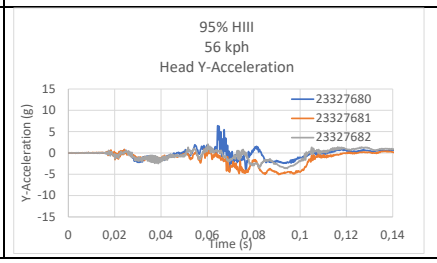
95% HIII
56 kph
Head Y-Acceleration
Y-Acceleration (g)
Time (s)
23327680
23327681
23327682

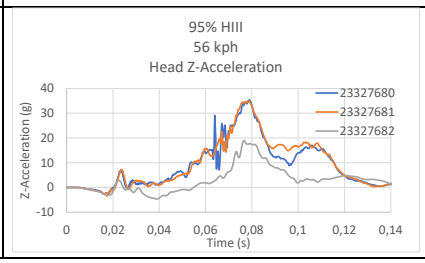
95% HIII
56 kph
Head Z-Acceleration
Z-Acceleration (g)
Time (s)
23327680
23327681
23327682

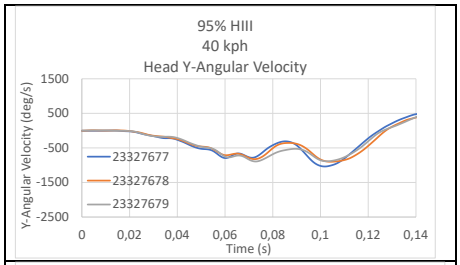
95% HIII
40 kph
Head Y-Angular Velocity
Y-Angular Velocity (deg/s)
Time (s)
23327677
23327678
23327679

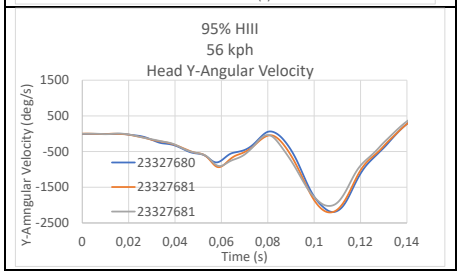
95% HIII
56 kph
Head Y-Angular Velocity
Y-Amngular Velocity (deg/s)
Time (s)
23327680
23327681
23327681

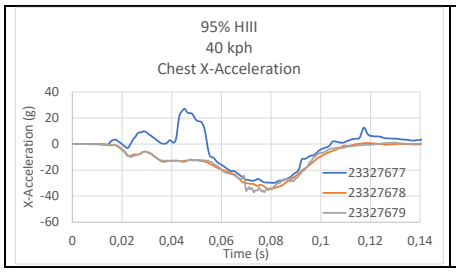
95% HIII
40 kph
Chest X-Acceleration
X-Acceleration (g)
Time (s)
23327677
23327678
23327679

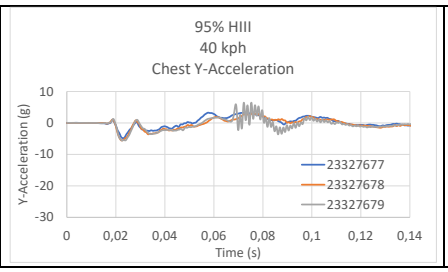
95% HIII
40 kph
Chest Y-Acceleration
Y-Acceleration (g)
Time (s)
23327677
23327678
23327679

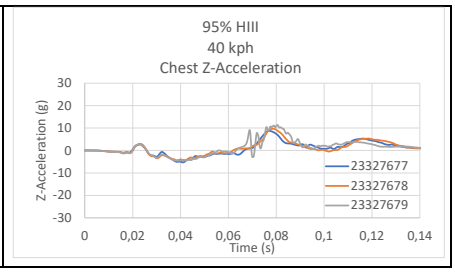
95% HIII
40 kph
Chest Z-Acceleration
Z-Acceleration (g)
Time (s)
23327677
23327678
23327679

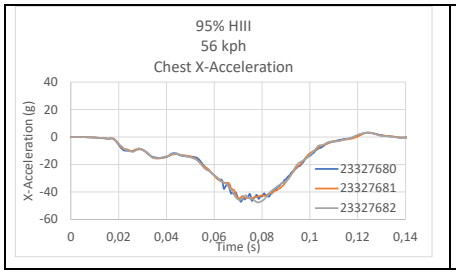
95% HIII
56 kph
Chest X-Acceleration
X-Acceleration (g)
Time (s)
23327680
23327681
23327682

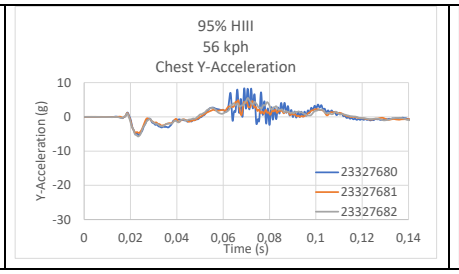
95% HIII
56 kph
Chest Y-Acceleration
Y-Acceleration (g)
Time (s)
23327680
23327681
23327682

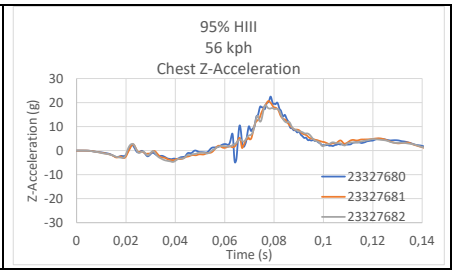
95% HIII
56 kph
Chest Z-Acceleration
Z-Acceleration (g)
Time (s)
23327680
23327681
23327682

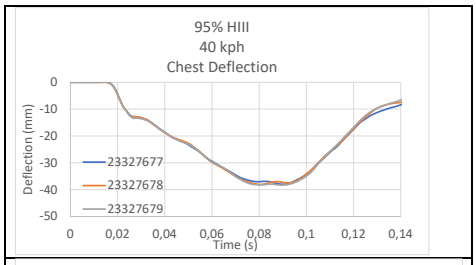
95% HIII
40 kph
Chest Deflection
Deflection (mm)
Time (s)
23327677
23327678
23327679

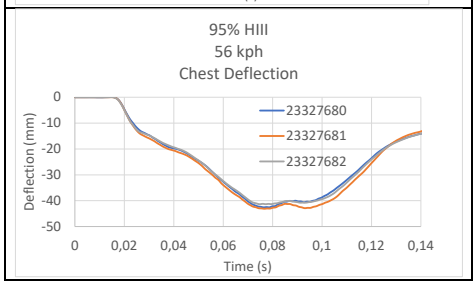
95% HIII
56 kph
Chest Deflection
Deflection (mm)
Time (s)
23327680
23327681
23327682

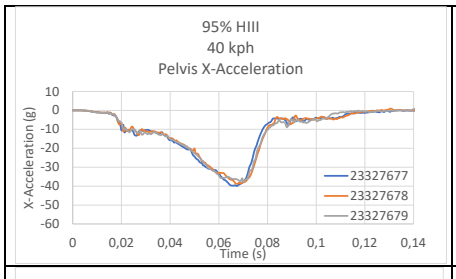
95% HIII
40 kph
Pelvis X-Acceleration
X-Acceleration (g)
Time (s)
23327677
23327678
23327679

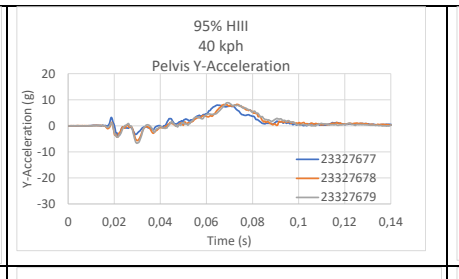
95% HIII
40 kph
Pelvis Y-Acceleration
Y-Acceleration (g)
Time (s)
23327677
23327678
23327679

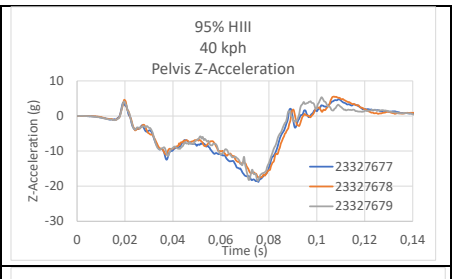
95% HIII
40 kph
Pelvis Z-Acceleration
Z-Acceleration (g)
Time (s)
23327677
23327678
23327679

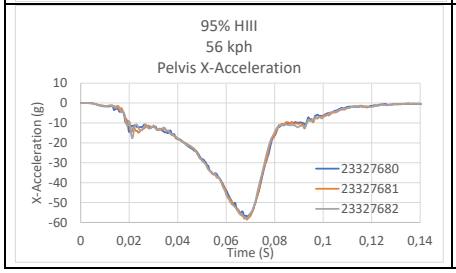
95% HIII
56 kph
Pelvis X-Acceleration
X-Acceleration (g)
Time (S)
23327680
23327681
23327682

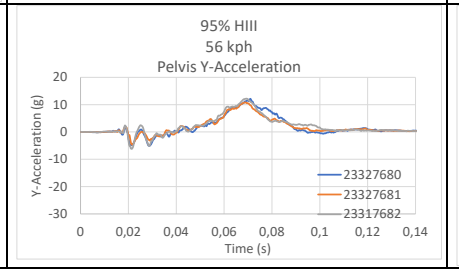
95% HIII
56 kph
Pelvis Y-Acceleration
Y-Acceleration (g)
Time (s)
23327680
23327681
23317682

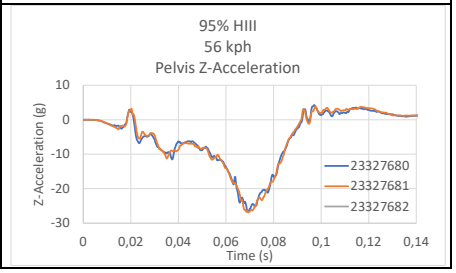
95% HIII
56 kph
Pelvis Z-Acceleration
Z-Acceleration (g)
Time (s)
23327680
23327681
23327682

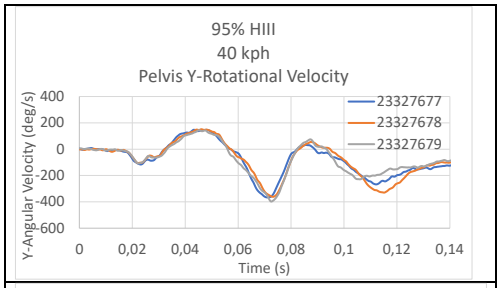
95% HIII
40 kph
Pelvis Y-Rotational Velocity
Y-Angular Velocity (deg/s)
Time (s)
23327677
23327678
23327679

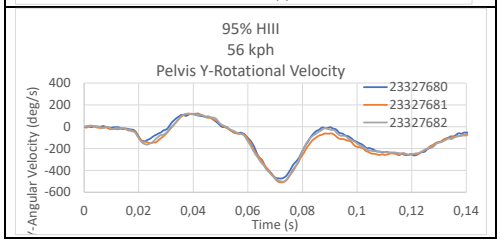
95% HIII
56 kph
Pelvis Y-Rotational Velocity
Time (s)
23327680
23327681
23327682

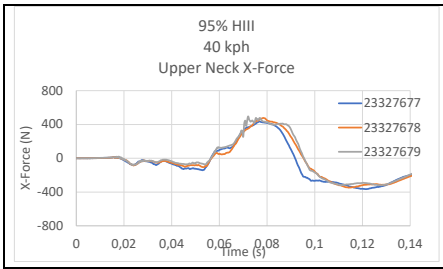
95% HIII
40 kph
Upper Neck X-Force
X-Force (N)
Time (s)
23327677
23327678
23327679

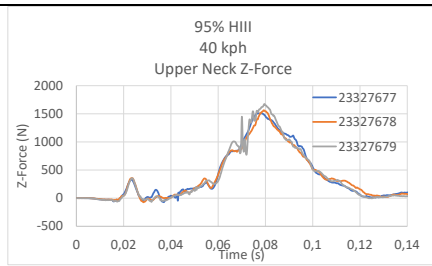
95% HIII
40 kph
Upper Neck Z-Force
Z-Force (N)
Time (s)
23327677
23327678
23327679

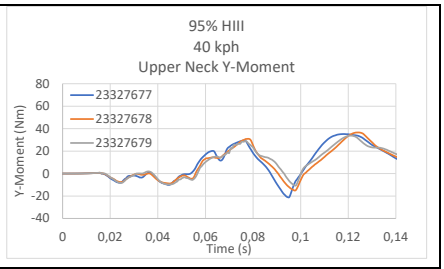
95% HIII
40 kph
Upper Neck Y-Moment
Y-Moment (Nm)
Time (s)
23327677
23327678
23327679

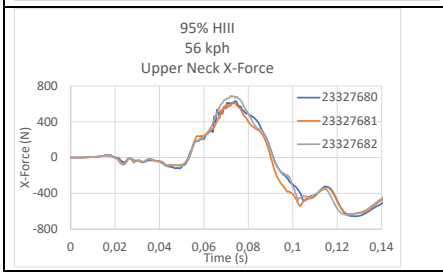
95% HIII
56 kph
Upper Neck X-Force
X-Force (N)
Time (s)
23327680
23327681
23327682

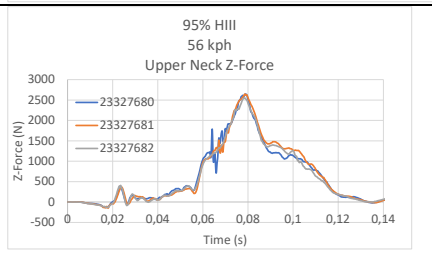
95% HIII
56 kph
Upper Neck Z-Force
Z-Force (N)
Time (s)
23327680
23327681
23327682

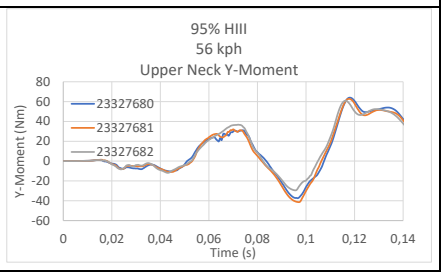
95% HIII
56 kph
Upper Neck Y-Moment
Y-Moment (Nm)
Time (s)
23327680
23327681
23327682

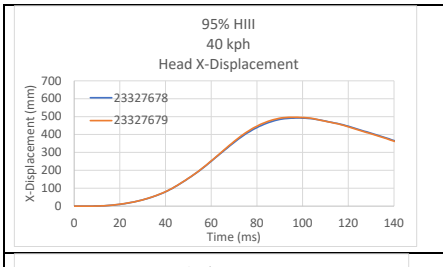
95% HIII
40 kph
Head X-Displacement
X-Displacement (mm)
Time (ms)
23327678
23327679

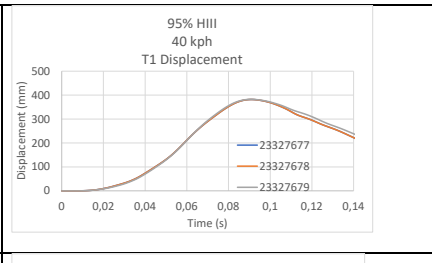
95% HIII
40 kph
T1 Displacement
Displacement (mm)
Time (s)
23327677
23327678
23327679

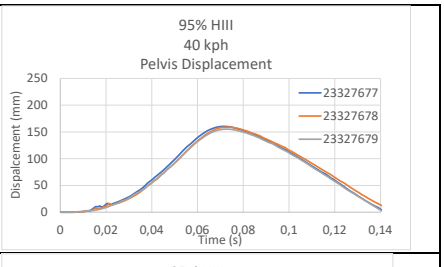
95% HIII
40 kph
Pelvis Displacement
Dispalcement (mm)
Time (s)
23327677
23327678
23327679

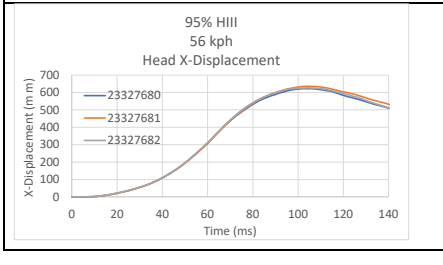
95% HIII
56 kph
Head X-Displacement
X-Displacement (m m)
Time (ms)
23327680
23327681
23327682

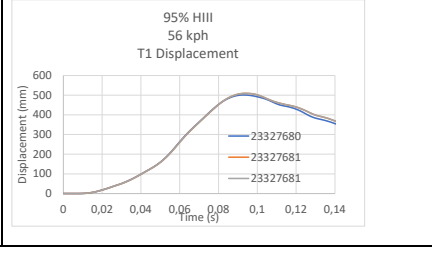
95% HIII
56 kph
T1 Displacement
Displacement (mm)
Time (s)
23327680
23327681
23327681

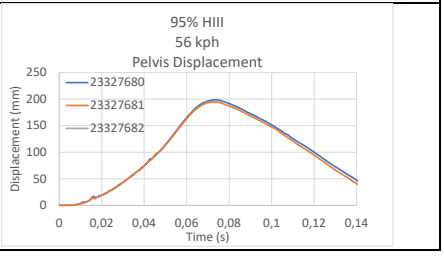
95% HIII
56 kph
Pelvis Displacement
Displacement (mm)
Time (s)
23327680
23327681
23327682

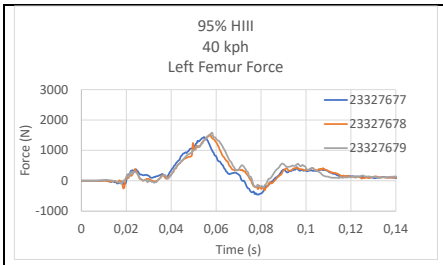
95% HIII
40 kph
Left Femur Force
Force (N)
Time (s)
23327677
23327678
23327679

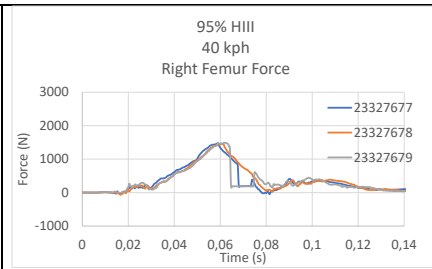
95% HIII
40 kph
Right Femur Force
Force (N)
Time (s)
23327677
23327678
23327679

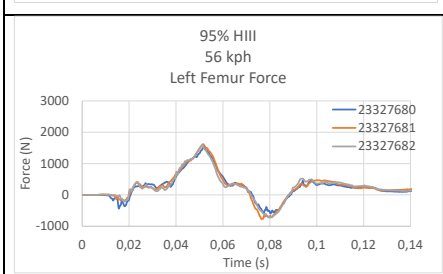
95% HIII
56 kph
Left Femur Force
Force (N)
Time (s)
23327680
23327681
23327682

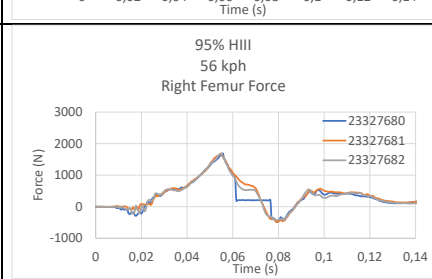
95% HIII
56 kph
Right Femur Force
Force (N)
Time (s)
23327680
23327681
23327682